

A FAMILY OF C^1 QUADRILATERAL FINITE ELEMENTS

MARIO KAPL, GIANCARLO SANGALLI, AND THOMAS TAKACS

ABSTRACT. We present a novel family of C^1 quadrilateral finite elements, which define global C^1 spaces over a general quadrilateral mesh with vertices of arbitrary valency. The elements extend the construction by Brenner and Sung [8], which is based on polynomial elements of tensor-product degree $p \geq 6$, to all degrees $p \geq 3$. Thus, we call the family of C^1 finite elements *Brenner-Sung quadrilaterals*. The proposed C^1 quadrilateral can be seen as a special case of the Argyris isogeometric element of [26]. The quadrilateral elements possess similar degrees of freedom as the classical Argyris triangles [1]. Just as for the Argyris triangle, we additionally impose C^2 continuity at the vertices. In this paper we focus on the lower degree cases, not covered in [8], that may be desirable for their lower computational cost and better conditioning of the basis: We consider indeed the polynomial quadrilateral of (bi-)degree 5, and the polynomial degrees $p = 3$ and $p = 4$ by employing a splitting into 3×3 or 2×2 polynomial pieces, respectively.

The proposed elements reproduce polynomials of total degree p . We show that the space provides optimal approximation order. Due to the interpolation properties, the error bounds are local on each element. In addition, we describe the construction of a simple, local basis and give for $p \in \{3, 4, 5\}$ explicit formulas for the Bézier or B-spline coefficients of the basis functions. Numerical experiments by solving the biharmonic equation demonstrate the potential of the proposed C^1 quadrilateral finite element for the numerical analysis of fourth order problems, also indicating that (for $p = 5$) the proposed element performs comparable or in general even better than the Argyris triangle with respect to the number of degrees of freedom.

1. INTRODUCTION

Using a standard Galerkin approach for the numerical analysis of high order problems, globally smooth function spaces are needed. E.g., for solving fourth order partial differential equations (PDEs) via the finite element method (FEM), C^1 finite element spaces are required. In the case of triangular meshes, two well-known examples are the Argyris element [1] and the Bell element [3]. Both elements require polynomials of degree $p \geq 5$, and are additionally C^2 at the vertices. While the normal derivative along an edge is of degree $p - 1$ for the Argyris element, its degree reduces to $p - 2$ for the Bell element. This leads for instance in case of polynomial degree $p = 5$ to the fact that the Argyris triangular space possesses six degrees of freedom for each vertex and one degree of freedom for each edge, while the Bell triangular space just has six degrees of freedom for each vertex and no additional degrees of freedom for the edges. For more details on the Argyris and Bell triangular element as well as on other C^1 triangular finite elements, we refer to

Date: May 12, 2020.

2010 Mathematics Subject Classification. Primary 65N30, secondary 65D07.

the books [7, 12]. C^1 finite element spaces of lower polynomial degree are in general based on splines, which are constructed over general triangulations, see [33].

The design of C^1 finite elements over quadrilateral meshes is in general more challenging compared to the case of triangular meshes, in particular with respect to the selection of the degrees of freedom. Examples of C^1 quadrilateral elements are [4, 6, 8, 34]. The Bogner-Fox-Schmit element [6] is a simple bivariate Hermite type C^1 construction which works for low polynomial degrees such as $p = 3$, but is limited to tensor-product meshes. In contrast, the C^1 elements [4, 8, 34] are applicable to more general quadrilateral meshes, but require a polynomial degree $p \geq 6$ in case of [8] and a polynomial degree $p \geq 5$ (for some specific settings just $p = 4$) in case of [4, 34]. The degrees of freedom for the finite element space [8] are selected similar to the Argyris triangular finite element space [1] by enforcing additionally C^2 -continuity at the vertices.

In contrast, the functions in [4, 34] are just C^1 at the vertices and the degrees of freedom are defined by means of the concept of minimal determining sets (cf. [33]), which is a common strategy for the construction of C^1 splines over triangular meshes, see also [33]. A different but related problem is the construction of C^1 function spaces over general quadrilateral meshes for the design of surfaces, such as in [18, 39, 40, 43]. The methods are based on the concept of geometric continuity [41], which is a well-known tool in computer aided geometric design for generating smooth complex surfaces.

An alternative to FEM is the use of isogeometric analysis (IgA), which was introduced in [20], and employs the same spline function space for describing the physical domain of interest and for representing the solution of the considered PDE, see e.g. [14, 20] for more details. In case of a single patch geometry, this allows the direct discretization of fourth order PDEs [47], such as the Kirchhoff-Love shells, e.g. [32, 31], the Navier-Stokes-Korteweg equation, e.g. [17], problems of strain gradient elasticity, e.g. [15, 38], or the Cahn-Hilliard equation, e.g. [16], by just using C^1 splines. In case of multi-patch geometries with possibly extraordinary vertices, i.e. vertices with a patch valency different to four, the design of smooth spline spaces is challenging and is the topic of current research.

Depending on the used type of parametrizations for the single patches of the given unstructured quadrilateral mesh, different techniques for the design of a C^1 spline space over this mesh have been developed. Possible examples in the case of planar, unstructured quadrilateral meshes are to use C^1 multi-patch parametrizations with a singularity at an extraordinary vertex, e.g. [37, 48], multi-patch parametrizations which are C^1 except in the vicinity of an extraordinary vertex, e.g. [28, 29, 30, 36], or multi-patch parametrizations which have to be just C^0 at all interfaces, e.g. [5, 10, 11, 13, 22, 23, 24, 26, 27, 35]. For more details about existing C^1 constructions for unstructured quadrilateral meshes, we refer to the recent survey article [25]. Beside this, in [9, 44, 46], different approaches for the construction of smooth spline functions of degree p are presented, which are C^s ($1 \leq s \leq p - 1$) everywhere, except in the vicinity of an extraordinary vertex, where they are just C^0 .

In this work, we present a family of C^1 quadrilateral finite elements, that are the low-degree (for $p \in \{3, 4, 5\}$) counterpart of the quadrilateral finite elements proposed in [8] (for $p \geq 6$) by Brenner and Sung. The interest for the low-degree case is that the computational cost for the linear system formation (due to numerical quadrature) and solution (that depends on the matrix conditioning) is more

favorable. We refer to these elements (the ones in [8] and the new ones) as *Brenner-Sung (BS) quadrilaterals*. These quadrilateral elements, in turn, are included in the isogeometric family of [26], and, indeed, the lower degrees $p \in \{3, 4\}$ construction is based on tensor-product splines.

The BS quadrilateral possesses similar degrees of freedom as the classical C^1 Argyris triangle [1]. An advantage of the quadrilateral construction over the triangular one is the simpler extension to the lower polynomial degrees $p = 3$ and $p = 4$ by just using tensor-product spline without the need of special splits for the mesh elements.

While in [26] the optimal approximation properties of the C^1 isogeometric spline space is just numerically shown, in this work the optimal approximation order of the BS quadrilateral space is proven. A further extension to [26] is that for some particular cases the Bézier or spline coefficients of the basis functions are explicitly given by simple formulas. Several numerical tests of solving the biharmonic equation also show the potential of the BS quadrilateral space for the numerical analysis of fourth order PDEs.

The outline of this paper is as follows. Section 2 introduces the quadrilateral mesh which will be used throughout the paper. In Section 3, the construction of the BS quadrilateral is described, focusing first on the bi-quintic polynomials, and then generalizing to splines, which allow the use of the lower polynomial degrees $p = 3$ and $p = 4$. Section 3 also discusses the connection of the BS quadrilateral with two well-known triangular finite elements, namely with the Argyris triangle [1] and with the Bell triangle [3]. In Section 4 we analyze the approximation properties of the BS quadrilateral space. Then, Sections 5 and 6 describe the design of local basis functions of the BS quadrilateral space for the case of polynomials and its extension for the case of splines, respectively, giving for the low-degree $p \in \{3, 4, 5\}$ cases the explicit Bézier and spline coefficients of the basis functions. The isoparametric extension of the BS quadrilateral, and its relation to the isogeometric element of [26], is briefly discussed in Section 7. Finally, we present in Section 8 numerical benchmarks on the biharmonic equation with different quadrilateral meshes, and conclude the paper in Section 9.

2. QUADRILATERAL MESH

We consider planar domains that allow meshing by quadrilaterals. Note that a generalization to domains with curved boundaries is possible with some additional care. We refer the reader to [4, 24], where such discretizations were developed, see also Section 7.

Let $\Omega \subset \mathbb{R}^2$ be an open, planar and connected region, which allows a quadrangulation, as defined below. This is the case if the boundary is piecewise linear, including all inner boundaries, if Ω is not simply connected. The coordinates in physical space are given as (x_1, x_2) . A quadrilateral mesh is a tuple

$$\mathcal{M} = (\mathcal{Q}, \mathcal{E}, \mathcal{V}),$$

consisting of a set of elements \mathcal{Q} , edges \mathcal{E} and vertices \mathcal{V} satisfying the following properties.

- Each vertex is a point in the plane, that is $\mathcal{V} \subset \mathbb{R}^2$.

- Each edge $\varepsilon \in \mathcal{E}$ is an open segment, and there exist two vertices $\mathbf{v}_1, \mathbf{v}_2 \in \mathcal{V}$ such that

$$\varepsilon = \{(1-s)\mathbf{v}_1 + s\mathbf{v}_2 : s \in]0, 1[\}.$$

- Each element $Q \in \mathcal{Q}$ is a convex, non-empty, open quadrilateral; there exist four vertices $\mathbf{v}_1, \dots, \mathbf{v}_4 \in \mathcal{V}$, four edges $\varepsilon_1, \dots, \varepsilon_4 \in \mathcal{E}$, with edge ε_i connecting \mathbf{v}_i with \mathbf{v}_{i+1} (modulo 4), given in counter-clockwise order; the element admits a parametrization by a $\mathbf{F}_Q : \widehat{Q} \rightarrow \overline{Q}$ which is bilinear on $\widehat{Q} = [0, 1]^2$, precisely:

$$(2.1) \quad \mathbf{F}_Q(\xi_1, \xi_2) = (1 - \xi_1)(1 - \xi_2)\mathbf{v}_1 + \xi_1(1 - \xi_2)\mathbf{v}_2 + \xi_1\xi_2\mathbf{v}_3 + (1 - \xi_1)\xi_2\mathbf{v}_4.$$

See Fig. 1 for a visualization.

- It holds

$$\overline{\Omega} = \bigcup_{Q \in \mathcal{Q}} \overline{Q}$$

and all intersections of different mesh elements are empty, i.e., for all $X, X' \in \mathcal{Q} \cup \mathcal{E} \cup \mathcal{V}$, with $X \neq X'$, we have $X \cap X' = \emptyset$.

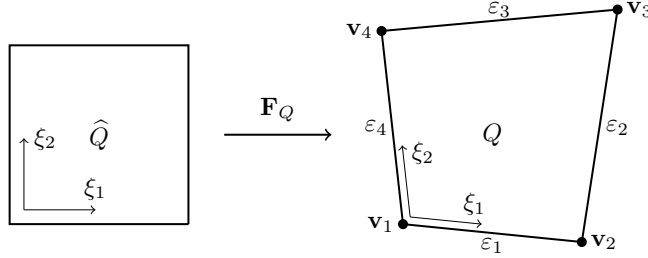


FIGURE 1. Visualization of the mapping \mathbf{F}_Q for a quadrilateral Q , with vertices, edges, parameter domain and local coordinates.

The last condition means that there are no hanging vertices in the quadrilateral mesh, i.e., all neighboring quadrilaterals share an entire edge or a vertex in their closure.

Given a $Q \in \mathcal{Q}$, we introduce the following notation: We denote by

$$\mathbf{t}^{(i)} = (t_1^{(i)}, t_2^{(i)})^T = \mathbf{v}_{i+1} - \mathbf{v}_i$$

the vector corresponding to the edge ε_i , and define

$$a^{(i)} = \det(\mathbf{t}^{(i-1)}, \mathbf{t}^{(i)}),$$

with indices modulo 4. Furthermore $h_{\varepsilon_i} = \|\mathbf{t}^{(i)}\|$ denotes the length of the corresponding edge ε_i , $h_Q = \max_i h_{\varepsilon_i}$, and ρ_Q its minimum angle defined as follows: If Q is a degenerate quadrilateral (that is a triangle) then $\rho_Q = 0$, otherwise ρ_Q is the minimum of the angles of the four triangles that are formed by the edges and the diagonals of Q . We assume however that each $Q \in \mathcal{Q}$ is non-degenerate, indeed the following holds.

Proposition 2.1. *For each $Q \in \mathcal{Q}$, for each $i = 1, \dots, 4$,*

$$(2.2) \quad 2\rho_Q \leq \angle(\mathbf{t}^{(i)}, \mathbf{t}^{(i-1)}) \leq \pi - 2\rho_Q,$$

and

$$(2.3) \quad c_1(\rho_Q) h_Q \leq h_{\varepsilon_i},$$

furthermore, for all $(\xi_1, \xi_2) \in \widehat{Q}$,

$$(2.4) \quad c_2(\rho_Q) h_Q^2 \leq \det(\nabla \mathbf{F}_Q(\xi_1, \xi_2)),$$

where $c_1(\rho_Q), c_2(\rho_Q) \in \mathbb{R}$ are constants that depend only on ρ_Q and are strictly positive for $\rho_Q > 0$.

Proof. Considering the split of Q into the four triangles formed by the edges and the diagonals, the bounds (2.2) on $\angle(\mathbf{t}^{(i)}, \mathbf{t}^{(i-1)})$ are straightforward. We also have, for $i \in \{1, 2, 3, 4\}$ (modulo 4),

$$\sin(\rho_Q) h_{\varepsilon_{i+1}} \leq h_{\varepsilon_i} \text{ and } \sin(\rho_Q) h_{\varepsilon_{i-1}} \leq h_{\varepsilon_i},$$

repeating the same argument twice

$$\sin^2(\rho_Q) h_{\varepsilon_{i+2}} \leq h_{\varepsilon_i},$$

therefore, for all $j \in \{1, 2, 3, 4\}$

$$\sin^2(\rho_Q) h_{\varepsilon_j} \leq h_{\varepsilon_i}$$

which gives the lower bound (2.3). We have by direct calculation

$$(2.5) \quad \nabla \mathbf{F}_Q(\xi_1, \xi_2) = \begin{bmatrix} \mathbf{t}^{(1)} - \xi_2(\mathbf{t}^{(1)} + \mathbf{t}^{(3)}) & -\mathbf{t}^{(4)} + \xi_1(\mathbf{t}^{(2)} + \mathbf{t}^{(4)}) \end{bmatrix}$$

and so, $\det(\nabla \mathbf{F}_Q)$ being a bilinear polynomial, its extrema are attained at the vertices of \widehat{Q} , that is

$$\min(\det(\nabla \mathbf{F}_Q)) = \min\{a^{(i)}, i = 1, \dots, 4\}.$$

Since

$$a^{(i)} = h_{\varepsilon_i} h_{\varepsilon_{i-1}} \sin(\angle(\mathbf{t}^{(i)}, \mathbf{t}^{(i-1)})),$$

the lower bound (2.4) follows from (2.2) and (2.3). \square

The condition $\rho_Q > 0$ also implies that the parametrization $\mathbf{F}_Q : \widehat{Q} \rightarrow \overline{Q}$ is regular, that is, its inverse $\mathbf{F}_Q^{-1} : \overline{Q} \rightarrow \widehat{Q}$ has bounded derivatives too. This follows from (2.4).

Similar to [8], we assume that the quadrilateral mesh \mathcal{M} is *shape regular*, that is

$$(2.6) \quad \rho = \inf_{Q \in \mathcal{Q}} \rho_Q > 0.$$

3. C^1 BS QUADRILATERAL ELEMENTS

In the following we recall the definition of BS quadrilaterals from [8], extend to the lower degree cases, and define the associated piecewise polynomial C^1 space over the domain of interest Ω , given a quadrilateral mesh \mathcal{M} . In our presentation we loosely follow the style of [7, 12]. The BS quadrilateral of degree $p \geq 5$ is constructed from bi-quintic polynomials with normal derivatives across interfaces that are polynomials of degree $p - 1$. For $p = 5$ the degrees of freedom are given as C^2 -data at the vertices, normal derivatives at the edge midpoints, as well as interior point evaluations. This is in accordance with the degrees of freedom of the Argyris triangle, see [1]. Moreover, one can define piecewise polynomial spaces of degree $p \in \{3, 4\}$, where the quadrilaterals have to be considered as macro-elements and subdivided further. This is explained in more detail in Section 6.

We denote with $\mathbb{P}^{(p,p)}$ the space of bivariate polynomials of bi-degree (p, p) and with \mathbb{P}^p the space of polynomials of total degree p , either uni- or bivariate, depending on context.

In the next subsections we introduce the local spaces and degrees of freedom corresponding to a single quadrilateral Q . To do this, we need the following notation.

Definition 3.1 (Pre-images of points and edges). For every point $\mathbf{v} \in \mathbb{R}^2$, with $\mathbf{v} \in \overline{Q}$, we define $\hat{\mathbf{v}}$ as the pre-image of \mathbf{v} under \mathbf{F}_Q , i.e., $\hat{\mathbf{v}} = \mathbf{F}_Q^{-1}(\mathbf{v})$. Analogously, we define $\hat{\varepsilon} = \mathbf{F}_Q^{-1}(\varepsilon)$ for $\varepsilon \in \mathcal{E}$ with $\varepsilon \subset \overline{Q}$. In Fig. 1 we have, e.g., $\hat{\mathbf{v}}_1 = (0, 0)^T$.

One set of degrees of freedom is the normal derivative at the edge midpoint, where we use the following notation. For every edge $\varepsilon \in \mathcal{E}$ between vertices \mathbf{v}_1 and \mathbf{v}_2 , let $\mathbf{m}_\varepsilon = \frac{1}{2}\mathbf{v}_1 + \frac{1}{2}\mathbf{v}_2$ be the edge midpoint. Moreover, let \mathbf{n}_ε be its unit normal vector and $\partial_{\mathbf{n}_\varepsilon}$ be the normal derivative of a function defined on Ω across the edge ε . Here we assume that the direction of the normal is fixed for every edge of the mesh \mathcal{M} .

3.1. Local space and degrees of freedom, $p = 5$. Given a quadrilateral $Q \in \mathcal{Q}$ we define the local function space and the local degrees of freedom as follows.

Definition 3.2 (BS quadrilateral for $p = 5$). Given a quadrilateral Q with vertices $\mathbf{v}_1, \mathbf{v}_2, \mathbf{v}_3$ and \mathbf{v}_4 and edges $\varepsilon_1, \varepsilon_2, \varepsilon_3$ and ε_4 following [12], we define the BS quadrilateral of degree $p = 5$ as (Q, P_Q^5, Λ_Q^5) , with

$$(3.1) \quad P_Q^5 = \left\{ \varphi : \overline{Q} \rightarrow \mathbb{R}, \text{ with } (\varphi \circ \mathbf{F}_Q) \in \mathbb{P}^{(5,5)}, (\partial_{\mathbf{n}_{\varepsilon_i}} \varphi \circ \mathbf{F}_Q)|_{\varepsilon_i} \in \mathbb{P}^4, 1 \leq i \leq 4 \right\}$$

and

$$(3.2) \quad \begin{aligned} \Lambda_Q^5 &= \Lambda_{0,Q} \cup \Lambda_{1,Q}^5 \cup \Lambda_{2,Q}^5, \text{ with} \\ \Lambda_{0,Q} &= \{ \varphi(\mathbf{v}_i), \partial_1 \varphi(\mathbf{v}_i), \partial_2 \varphi(\mathbf{v}_i), \partial_1 \partial_1 \varphi(\mathbf{v}_i), \partial_1 \partial_2 \varphi(\mathbf{v}_i), \partial_2 \partial_2 \varphi(\mathbf{v}_i), 1 \leq i \leq 4 \}, \\ \Lambda_{1,Q}^5 &= \{ \partial_{\mathbf{n}_{\varepsilon_i}} \varphi(\mathbf{m}_{\varepsilon_i}), 1 \leq i \leq 4 \}, \\ \Lambda_{2,Q}^5 &= \{ \varphi(\mathbf{x}), \mathbf{x} \in \mathcal{F}_Q^5 \}. \end{aligned}$$

The set of face points is given as

$$\mathcal{F}_Q^5 = \left\{ \mathbf{F}_Q(\eta_1, \eta_2), \eta_1, \eta_2 \in \left\{ \frac{2}{5}, \frac{3}{5} \right\} \right\}.$$

See Fig. 2 for a visualization of the local degrees of freedom of the BS quadrilateral.

The unisolvency of the degrees of freedom Λ_Q^5 for the space P_Q^5 follows from the basis construction in Section 5.

We have already observed the similarity of this construction with the Argyris triangle. Let us recall the definition of the Argyris triangle for $p = 5$ as given in [1, 12].

Definition 3.3 (Argyris triangle for $p = 5$). Given a triangle T with vertices $\mathbf{v}_1, \mathbf{v}_2$ and \mathbf{v}_3 and edges $\varepsilon_1, \varepsilon_2$ and ε_3 we define the Argyris triangle as (T, P_T, Λ_T) , with $P_T = \mathbb{P}^5$ and $\Lambda_T = \Lambda_{0,T} \cup \Lambda_{1,T}$, with

$$\begin{aligned} \Lambda_{0,T} &= \{ \varphi(\mathbf{v}_i), \partial_1 \varphi(\mathbf{v}_i), \partial_2 \varphi(\mathbf{v}_i), \partial_1 \partial_1 \varphi(\mathbf{v}_i), \partial_1 \partial_2 \varphi(\mathbf{v}_i), \partial_2 \partial_2 \varphi(\mathbf{v}_i), 1 \leq i \leq 3 \}, \\ \Lambda_{1,T} &= \{ \partial_{\mathbf{n}_{\varepsilon_i}} \varphi(\mathbf{m}_{\varepsilon_i}), 1 \leq i \leq 3 \}. \end{aligned}$$

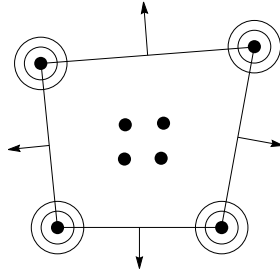


FIGURE 2. The BS quadrilateral for $p = 5$, visualizing the degrees of freedom Λ_Q^5 .

Hence, the degrees of freedom for the BS quadrilateral ($p = 5$) and Argyris triangle ($p = 5$) are the same, except for the additional point evaluations at face points in the quadrilateral case. In addition, the traces as well as normal derivatives along edges are the same in both elements, i.e., for $p = 5$ traces are quintic polynomials and normal derivatives are quartic polynomials. The degrees of freedom for the Argyris triangle are visualized in Figure 3 (left).

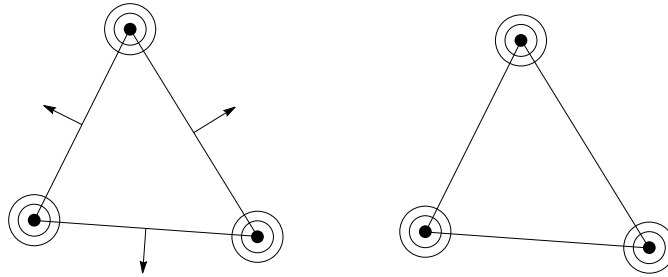


FIGURE 3. The Argyris triangle (left) and Bell triangle (right), visualizing Λ_T^A and Λ_T^B , respectively.

In addition, the condition that the normal derivative along an edge is of degree 4, is similar to the condition on the Bell triangular element [3], a quintic element, where normal derivatives are assumed to be polynomials of degree 3, thus eliminating the normal derivative degrees of freedom and resulting in 18 degrees of freedom per triangle.

Definition 3.4 (Bell triangle for $p = 5$). Given a triangle T with vertices \mathbf{v}_1 , \mathbf{v}_2 and \mathbf{v}_3 and edges ε_1 , ε_2 and ε_3 we define the Bell triangle as (T, P_T^B, Λ_T^B) , with

$$(3.3) \quad P_T^B = \{ \varphi : \bar{T} \rightarrow \mathbb{R}, \text{ with } \varphi \in \mathbb{P}^5, \partial_{\mathbf{n}_{\varepsilon_i}} \varphi|_{\varepsilon_i} \in \mathbb{P}^3, 1 \leq i \leq 3 \}$$

and $\Lambda_T^B = \Lambda_{0,T}$.

The degrees of freedom for the Bell triangle are visualized in Figure 3 (right). Both triangle elements possess variants of higher degree, see [1, 3, 12, 33]. For triangular elements, constructions of smooth spaces for lower degrees are usually based on special splits, such as the Clough-Tocher or Powell-Sabin 6- or 12-splits. Unlike the triangular case, in the quadrilateral case variants of lower degree are relatively straightforward and follow from the spline constructions developed in [26].

3.2. Local space and degrees of freedom, $p \geq 6$. Given a quadrilateral $Q \in \mathcal{Q}$ we define the local function space and the local degrees of freedom for $p \geq 6$ as follows.

Definition 3.5 (BS quadrilateral [8]). Given a quadrilateral Q with vertices $\mathbf{v}_1, \mathbf{v}_2, \mathbf{v}_3$ and \mathbf{v}_4 and edges $\varepsilon_1, \varepsilon_2, \varepsilon_3$ and ε_4 we define the BS quadrilateral of degree $p \geq 6$ as (Q, P_Q^p, Λ_Q^p) , with

$$(3.4) \quad P_Q^p = \left\{ \varphi : \overline{Q} \rightarrow \mathbb{R}, \text{ with } (\varphi \circ \mathbf{F}_Q) \in \mathbb{P}^{(p,p)}, (\partial_{\mathbf{n}_{\varepsilon_i}} \varphi \circ \mathbf{F}_Q)|_{\varepsilon_i} \in \mathbb{P}^{p-1}, 1 \leq i \leq 4 \right\}$$

and

$$(3.5) \quad \begin{aligned} \Lambda_Q^p &= \Lambda_{0,Q} \cup \Lambda_{1,Q}^p \cup \Lambda_{2,Q}^p, \text{ with} \\ \Lambda_{0,Q} &= \{ \varphi(\mathbf{v}_i), \partial_1 \varphi(\mathbf{v}_i), \partial_2 \varphi(\mathbf{v}_i), \partial_1 \partial_1 \varphi(\mathbf{v}_i), \partial_1 \partial_2 \varphi(\mathbf{v}_i), \partial_2 \partial_2 \varphi(\mathbf{v}_i), 1 \leq i \leq 4 \}, \\ \Lambda_{1,Q}^p &= \left\{ \varphi(\mathbf{F}_{\varepsilon_i}(\frac{j}{p})), \text{ for } 1 \leq i \leq 4, 3 \leq j \leq p-3 \right\} \\ &\quad \cup \left\{ \partial_{\mathbf{n}_{\varepsilon_i}} \varphi(\mathbf{F}_{\varepsilon_i}(\frac{j}{p-1})), \text{ for } 1 \leq i \leq 4, 2 \leq j \leq p-3 \right\}, \\ \Lambda_{2,Q}^p &= \left\{ \varphi(\mathbf{x}), \mathbf{x} \in \mathcal{F}_Q^p \right\}. \end{aligned}$$

Here $\mathbf{F}_{\varepsilon_i} = \mathbf{F}_Q|_{\varepsilon_i}$, and the set of face points is given as

$$\mathcal{F}_Q^p = \left\{ \mathbf{F}_Q(\eta_1, \eta_2), \eta_1, \eta_2 \in \left\{ \frac{2}{p}, \dots, \frac{p-2}{p} \right\} \right\}.$$

As one can easily see, Definition 3.5 covers also the case of Definition 3.2. Obviously, we have the following. The degrees of freedom Λ_Q^p are unisolvent for the space P_Q^p . Indeed, one can show (see [8]) that the dimension of P_Q^p is given by $\dim(\mathbb{P}^{(p,p)}) = (p+1)^2$ minus the number of constraints from $(\partial_{\mathbf{n}_{\varepsilon_i}} \varphi \circ \mathbf{F}_Q)|_{\varepsilon_i} \in \mathbb{P}^{p-1}$, which are one per edge, that is, four. Then the dimension of P_Q^p is $(p+1)^2 - 4$ and equals the cardinality of Λ_Q^p .

3.3. Local space and degrees of freedom, $p \in \{3, 4\}$. In the following we extend the construction on quadrilaterals to lower degrees $p = 3$ and $p = 4$ using a split into sub-elements, as in Fig. 4. We assume that the parameter domain \widehat{Q} is split into sub-elements $\hat{q} \in s_k(\widehat{Q})$, with

$$(3.6) \quad s_k(\widehat{Q}) = \left\{ \left[\frac{i}{k}, \frac{i+1}{k} \right] \times \left[\frac{j}{k}, \frac{j+1}{k} \right], 0 \leq i \leq k-1, 0 \leq j \leq k-1 \right\}.$$

Definition 3.6 (C^1 quadrilateral macro-element for $p \in \{3, 4\}$). Given a quadrilateral Q with vertices $\mathbf{v}_1, \mathbf{v}_2, \mathbf{v}_3$ and \mathbf{v}_4 and edges $\varepsilon_1, \varepsilon_2, \varepsilon_3$ and ε_4 we define the C^1 quadrilateral macro-element of degree $p \in \{3, 4\}$ as (Q, P_Q^p, Λ_Q^p) , with

$$(3.7) \quad P_Q^p = \left\{ \varphi : Q \rightarrow \mathbb{R}, \text{ with } \begin{array}{ll} \varphi & \in C^{p-2}(Q), \\ (\varphi \circ \mathbf{F}_Q)|_{\hat{q}} & \in \mathbb{P}^{(p,p)}, \quad \text{for } \hat{q} \in s_{6-p}(\widehat{Q}), \\ (\varphi \circ \mathbf{F}_Q)|_{\varepsilon_i} & \in C^{p-1}(\hat{\varepsilon}_i), \quad \text{for } 1 \leq i \leq 4, \\ (\partial_{\mathbf{n}_{\varepsilon_i}} \varphi \circ \mathbf{F}_Q)|_{\varepsilon_i \cap \hat{q}} & \in \mathbb{P}^{p-1} \end{array} \right\}$$

and

(3.8)

$$\Lambda_Q^p = \Lambda_{0,Q} \cup \Lambda_{1,Q}^p \cup \Lambda_{2,Q}^p, \text{ with}$$

$$\Lambda_{0,Q} = \{\varphi(\mathbf{v}_i), \partial_1 \varphi(\mathbf{v}_i), \partial_2 \varphi(\mathbf{v}_i), \partial_1 \partial_1 \varphi(\mathbf{v}_i), \partial_1 \partial_2 \varphi(\mathbf{v}_i), \partial_2 \partial_2 \varphi(\mathbf{v}_i), 1 \leq i \leq 4\},$$

$$\Lambda_{1,Q}^p = \{\partial_{\mathbf{n}_{\varepsilon_i}} \varphi(\mathbf{m}_{\varepsilon_i}), 1 \leq i \leq 4\},$$

$$\Lambda_{2,Q}^p = \{\varphi(\mathbf{x}), \mathbf{x} \in \mathcal{F}_Q^p\}.$$

For $p = 4$ the set of face points is given as

$$\mathcal{F}_Q^4 = \left\{ \mathbf{F}_Q(\eta_1, \eta_2), \quad \eta_1, \eta_2 \in \left\{ \frac{1}{4}, \frac{2}{4}, \frac{3}{4} \right\} \right\},$$

for $p = 3$ we have

$$\mathcal{F}_Q^3 = \left\{ \mathbf{F}_Q(\eta_1, \eta_2), \quad \eta_1, \eta_2 \in \left\{ \frac{2}{9}, \frac{4}{9}, \frac{5}{9}, \frac{7}{9} \right\} \right\}.$$

As for $p = 5$, the degrees of freedom Λ_Q^p completely determine the functions from the space P_Q^p and the dimension is given by $\dim(P_Q^p) = |\Lambda_Q^p| = 28 + (7 - p)^2$. This follows as a special case of Lemma 6.2.

In Fig. 4 we visualize the polynomial sub-elements from (3.7) and local degrees of freedom from (3.8) for $p \in \{3, 4\}$.

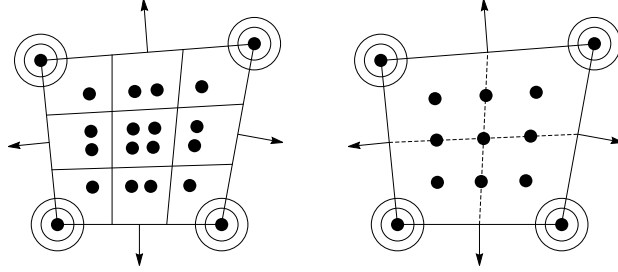


FIGURE 4. The C^1 quadrilateral macro-elements for $p = 3$ (left) and $p = 4$ (right), visualizing Λ_Q^3 and Λ_Q^4 , respectively. The solid inner lines represent lines of C^1 continuity, whereas the dashed lines are C^2 .

3.4. Global space and global degrees of freedom. In this section we describe the global space and set of degrees of freedom from the local spaces and degrees of freedom defined above, with focus on the low-degree cases $p \in \{3, 4, 5\}$.

Definition 3.7 (Global degrees of freedom). Let $p \in \{3, 4, 5\}$. Given a quadrilateral mesh \mathcal{M} we have the degrees of freedom Λ^p , given as

- $\varphi(\mathbf{v}), \partial_1 \varphi(\mathbf{v}), \partial_2 \varphi(\mathbf{v}), \partial_1 \partial_1 \varphi(\mathbf{v}), \partial_1 \partial_2 \varphi(\mathbf{v})$ and $\partial_2 \partial_2 \varphi(\mathbf{v})$ for all vertices $\mathbf{v} \in \mathcal{V}$;
- $\partial_{\mathbf{n}_\varepsilon} \varphi(\mathbf{m}_\varepsilon)$ for all edge midpoints \mathbf{m}_ε with $\varepsilon \in \mathcal{E}$; and
- $\varphi(\mathbf{x}_Q)$ for all face points $\mathbf{x}_Q \in \mathcal{F}_Q^p$ for all $Q \in \mathcal{Q}$.

The global degrees of freedom in Definition 3.7 together with the finite element descriptions in Definitions 3.2 and 3.6 determine a global space $\mathcal{S}^p(\mathcal{M}) \subset C^1(\Omega)$.

Lemma 3.8 (The C^1 quadrilateral space). *Let $p \in \{3, 4, 5\}$ and let \mathcal{M} of Ω and let the space $\mathcal{S}^p(\mathcal{M})$ be given by the degrees of freedom Λ^p as in Definition 3.7, with*

$$\mathcal{S}^p(\mathcal{M})|_Q = P_Q^p \text{ for all } Q \in \mathcal{Q},$$

where the local spaces P_Q^p are given as in Definition 3.2 or 3.6, respectively. Then the global space satisfies $\mathcal{S}^p(\mathcal{M}) \subset C^1(\Omega)$ and we have

$$\dim(\mathcal{S}^p(\mathcal{M})) = |\Lambda^p| = (7 - p)^2 \cdot |\mathcal{Q}| + 1 \cdot |\mathcal{E}| + 6 \cdot |\mathcal{V}|.$$

Proof. Note that the piecewise polynomial space P_Q^p from Definition 3.6 covers also the polynomial case $p = 5$ for $k = 1$, where $s_{6-p}(\hat{Q}) = s_1(\hat{Q}) = \{\hat{Q}\}$. To prove $\mathcal{S}^p(\mathcal{M}) \subset C^1(\Omega)$ we consider all C^1 -data along a single edge ε between two elements Q and Q' . Let $\varphi \in \mathcal{S}^p(\mathcal{M})$ and let $\hat{q} \in s_{6-p}(\hat{Q})$. We have, since $\varphi|_Q \in P_Q^p$, that $(\varphi \circ \mathbf{F}_Q)|_{\varepsilon \cap \hat{q}} \in \mathbb{P}^p$ and $(\varphi \circ \mathbf{F}_Q)|_{\varepsilon} \in C^{p-1}$, and $(\partial_{\mathbf{n}_\varepsilon} \varphi \circ \mathbf{F}_Q)|_{\varepsilon \cap \hat{q}} \in \mathbb{P}^{p-1}$. Consequently, since $\mathbf{F}_Q|_{\varepsilon}$ is a linear function, we have $\varphi|_{\varepsilon \cap q} \in \mathbb{P}^p$, $\varphi|_{\varepsilon} \in C^{p-1}$ and $\partial_{\mathbf{n}_\varepsilon} \varphi|_{\varepsilon \cap q} \in \mathbb{P}^{p-1}$, where $\varepsilon \cap q = \varepsilon \cap \mathbf{F}_Q(\hat{q}) = \varepsilon \cap \mathbf{F}_{Q'}(\hat{q}')$. Hence, $\varphi|_{\varepsilon}$ is a piecewise polynomial of degree p , with dimension 6. Value, first and second derivative (in direction of the edge) of φ at the two vertices of ε are determined by the C^2 -data. The function $\varphi|_{\varepsilon}$ is thus completely determined by the C^2 -data. This is independent of the element Q, Q' under consideration. Hence, we have $\varphi \in C^0(\Omega)$. Moreover, by definition, the function $\partial_{\mathbf{n}_\varepsilon} \varphi|_{\varepsilon}$ is a piecewise polynomial of degree $p - 1$, with dimension 5, independent of Q, Q' . Of those 5 degrees of freedom, the C^2 -data at the vertices determine two each, whereas one is determined by $\partial_{\mathbf{n}_\varepsilon} \varphi(\mathbf{m}_\varepsilon)$. Hence, $\varphi|_{\varepsilon}$ and $\partial_{\mathbf{n}_\varepsilon} \varphi|_{\varepsilon}$ are completely determined by the global degrees of freedom and $\varphi \in C^1(\Omega)$. What remains to be shown is that $\dim(\mathcal{S}^p(\mathcal{M})) = |\Lambda^p|$. Its proof follows directly from a simple counting argument. \square

We have presented Lemma 3.8 and its proof purely in terms of a finite element setting, considering the local spaces and global degrees of freedom. See [26, Section 4] for a more general statement on spline patches. Note that the space $\mathcal{S}^p(\mathcal{M})$ is C^2 at all vertices by construction.

Remark 3.9. Since both the degrees of freedom Λ_Q^p as well as the definition of the local space P_Q^p depend on derivatives in normal direction, the proposed BS quadrilaterals (including the macro-element variants) are not affine invariant, as the Argyris triangle, which possesses an affine invariant space, but no affine invariant degrees of freedom.

4. APPROXIMATION PROPERTIES

In this section we prove local and global approximation estimates, where the error is measured only in the norms of interest $\|\cdot\|_{L^\infty}$, $\|\cdot\|_{L^2}$, and $\|\cdot\|_{H^\ell}$, for simplicity. For the notation concerning Sobolev spaces, we follow [7].

Given a convex quadrilateral $Q \in \mathcal{Q}$, the main ingredient to prove the local approximation estimate is the projector $\Pi_{P_Q^p} : C^2(\bar{Q}) \rightarrow P_Q^p$ defined by

$$(4.1) \quad \Pi_{P_Q^p}(\varphi) = \sum_{\lambda_Q \in \Lambda_Q^p} \lambda_Q(\varphi) \beta_{\lambda_Q},$$

where $\beta_{\lambda_Q} \in P_Q^p$ are basis functions that satisfy $\lambda_Q(\beta_{\lambda_Q}) = 1$ and $\lambda'_Q(\beta_{\lambda_Q}) = 0$ for all $\lambda_Q \neq \lambda'_Q \in \Lambda_Q^p$. The existence of such a basis is a consequence of the unisolvence

of the set of degrees of freedom Λ_Q^p . A key property for the approximation result is the basis stability stated below.

Lemma 4.1. *Let $Q \in \mathcal{Q}$ be a convex quadrilateral. There exists a constant $C > 0$, dependent on h_Q , ρ_Q , and p such that for all $\lambda_Q \in \Lambda_Q^p$*

$$\|\beta_{\lambda_Q}\| \leq C$$

where $\|\cdot\|$ is any of the norms of interest.

Proof. Each basis function β_{λ_Q} can be obtained by imposing the conditions to belong to the space

$$(4.2) \quad \beta_{\lambda_Q} \in P_Q^p$$

and to be in duality to the degrees of freedom

$$(4.3) \quad \lambda_Q(\beta_{\lambda_Q}) = 1 \text{ and } \lambda'_Q(\beta_{\lambda_Q}) = 0, \quad \forall \lambda_Q \neq \lambda'_Q \in \Lambda_Q^p.$$

In parametric coordinates, it means that $\beta_{\lambda_Q} \circ \mathbf{F}_Q$ defined on \widehat{Q} is a polynomial (for $p \geq 5$, it belongs to $\mathbb{P}^{(p,p)}$) or piecewise polynomial (for $p \in \{3, 4\}$, its restriction to each subelement $\hat{q} \in s_{6-p}(\widehat{Q})$ belongs to $\mathbb{P}^{(p,p)}$) that fulfills (4.2)–(4.3). These conditions above involve the first and second derivatives of the inverse parametrization \mathbf{F}_Q^{-1} , that are well defined and bounded on \widehat{Q} thanks to (2.4). Recalling the expression (2.5) of $\nabla \mathbf{F}_Q$, the first and second derivatives of \mathbf{F}_Q^{-1} are rational polynomials in x_1 and x_2 and depend continuously on the parameters $\mathbf{t}^{(1)}, \dots, \mathbf{t}^{(4)}$. Therefore $\|\beta_{\lambda_Q}\|$ only depends on $\mathbf{t}^{(1)}, \dots, \mathbf{t}^{(4)}$, the dependence is continuous and the parameters belong to the compact set

$$\left\{ \mathbf{t}^{(1)}, \dots, \mathbf{t}^{(4)} : 2\rho_Q \leq \angle(\mathbf{t}^{(i)}, \mathbf{t}^{(i-1)}) \leq \pi - 2\rho_Q \text{ and } \|\mathbf{t}^{(i)}\| \leq h_Q \right\},$$

thanks to Proposition 2.1. Continuity and compactness give the existence of a maximum of $\|\beta_{\lambda_Q}\|$ which only depends on h_Q , ρ_Q and on p . \square

Lemma 4.1 yields the local stability of the projector.

Lemma 4.2. *Let $Q \in \mathcal{Q}$ be any convex quadrilateral. There exists a constant $C > 0$, dependent on h_Q , ρ_Q , and p such that for all $\psi \in C^2(\overline{Q})$,*

$$\|\Pi_{P_Q^p} \psi\| \leq C \|\psi\|_{C^2(\overline{Q})},$$

where $\|\cdot\|$ is one of the norms of interest.

Proof. Thanks to Lemma 4.1, we have that

$$\|\Pi_{P_Q^p} \psi\| \leq C \max_{\lambda \in \Lambda_Q^p} |\lambda(\psi)|,$$

and then we use the obvious continuity $|\lambda(\psi)| \leq \|\psi\|_{C^2(\overline{Q})}$. \square

The next two Lemmata, from [7], concern standard Sobolev inequalities and standard polynomial approximation over $Q \in \mathcal{Q}$.

Lemma 4.3 ([7, Lemma 4.3.4]). *Let $Q \in \mathcal{Q}$ be any convex quadrilateral. There exists a constant $C_{SI} > 0$, dependent on h_Q and ρ_Q such that for all $\psi \in H^4(Q)$ we have $\psi \in C^2(Q)$ and*

$$\|\psi\|_{C^2(\overline{Q})} \leq C_{SI} \|\psi\|_{H^4(Q)}.$$

Lemma 4.4 ([7, Lemma 4.3.8]). *Let $Q \in \mathcal{Q}$ be any convex quadrilateral and B a maximal ball inscribed in Q . Let $m \leq p + 1$. There exists a constant $C_{BH} > 0$, dependent on h_Q , ρ_Q , and p such that for all $\varphi \in H^m(Q)$*

$$\|\varphi - \Pi_{\mathbb{P}^p} \varphi\|_{H^m(Q)} \leq C_{BH} |\varphi|_{H^m(Q)},$$

where $\Pi_{\mathbb{P}^p} \varphi$ is the averaged Taylor polynomial of degree p of φ over B .

The last property we need is that the BS quadrilateral element space contains the polynomials of total degree p .

Lemma 4.5. *Let $Q \in \mathcal{Q}$ be any convex quadrilateral, then $\mathbb{P}^p \subset P_Q^p$.*

Proof. Let $\psi \in \mathbb{P}^p$, we need to show that $\psi \circ \mathbf{F}_Q \in \mathbb{P}^{(p,p)}$ and $(\partial_{\mathbf{n}_{\varepsilon_i}} \psi \circ \mathbf{F}_Q)|_{\varepsilon_i} \in \mathbb{P}^{p-1}$ for all ε_i , according to (3.1) and (3.7). Note that we do not need to consider the sub-elements separately, as ψ is a global polynomial. The composition of a polynomial of total degree p with a bilinear function always results in a polynomial of bi-degree (p,p) , hence we have $\psi \circ \mathbf{F}_Q \in \mathbb{P}^{(p,p)}$. Moreover, the directional derivative $\partial_{\mathbf{n}_{\varepsilon_i}} \psi$ is a polynomial of total degree $p - 1$, restricted to an edge yields a univariate polynomial of degree $p - 1$, which gives $(\partial_{\mathbf{n}_{\varepsilon_i}} \psi \circ \mathbf{F}_Q)|_{\varepsilon_i} \in \mathbb{P}^{p-1}$ since $\mathbf{F}_Q|_{\varepsilon_i}$ is a linear parametrization. \square

We can now state and prove the local approximation estimate.

Theorem 4.6. *Let $Q \in \mathcal{Q}$ be a convex quadrilateral. There exists a constant $C > 0$, dependent on ρ_Q and on p , such that for $0 \leq \ell \leq 2$, $4 \leq m \leq p + 1$ and for all $\varphi \in H^m(Q)$ we have*

$$\left| \varphi - \Pi_{P_Q^p} \varphi \right|_{H^\ell(Q)} \leq C h_Q^{m-\ell} |\varphi|_{H^m(Q)};$$

moreover, for $3 \leq m \leq p + 1$, $3 \leq p$ and for all $\varphi \in W_\infty^m(Q)$,

$$\left\| \varphi - \Pi_{P_Q^p} \varphi \right\|_{L^\infty(Q)} \leq C h_Q^m |\varphi|_{W_\infty^m(Q)}.$$

Proof. The proof follows the proof of [7, Theorem 4.4.4]. We can assume $h_Q = 1$, since the general case and the role of h_Q in the estimates follow by an homogeneity argument. We have

$$\begin{aligned} \|\varphi - \Pi_{P_Q^p} \varphi\|_{H^\ell(Q)} &\leq \|\varphi - \Pi_{\mathbb{P}^p} \varphi\|_{H^\ell(Q)} + \|\Pi_{\mathbb{P}^p} \varphi - \Pi_{P_Q^p} \varphi\|_{H^\ell(Q)} \\ &= \|\varphi - \Pi_{\mathbb{P}^p} \varphi\|_{H^\ell(Q)} + \|\Pi_{P_Q^p}(\Pi_{\mathbb{P}^p} \varphi - \varphi)\|_{H^\ell(Q)} \end{aligned}$$

Applying the bound from Lemma 4.2, Lemma 4.3 and 4.4, we obtain

$$\begin{aligned} \|\varphi - \Pi_{P_Q^p} \varphi\|_{H^\ell(Q)} &\leq \|\varphi - \Pi_{\mathbb{P}^p} \varphi\|_{H^\ell(Q)} + C \|\varphi - \Pi_{\mathbb{P}^p} \varphi\|_{C^2(\bar{Q})} \\ &\leq (1 + CC_{SI}) \|\varphi - \Pi_{\mathbb{P}^p} \varphi\|_{H^m(Q)} \\ &\leq (1 + CC_{SI}) C_{BH} |\varphi|_{H^m(Q)}, \end{aligned}$$

The L^∞ -estimate follows the same idea as the H^ℓ -estimates, where a bound of the form

$$\|\Pi_{S(\mathcal{M})}(\varphi)\|_{L^\infty(Q)} \leq \sigma(\rho, p) \|\varphi\|_{C^2(\bar{Q})}$$

is needed together with estimates similar to Lemma 4.3 and 4.4. Note that in case of the L^∞ estimate we only need $m \geq 3$, see again [7, Theorem 4.4.4]. \square

From this local error estimate, a global estimate follows straightforwardly. Let $\Pi_{\mathcal{S}^p(\mathcal{M})} : C^2(\bar{\Omega}) \rightarrow \mathcal{S}^p(\mathcal{M})$ be the global projector defined as

$$(4.4) \quad \Pi_{\mathcal{S}^p(\mathcal{M})}\varphi = \sum_{\lambda \in \Lambda^p} \lambda(\varphi)\beta_\lambda,$$

where each $\beta_\lambda \in \mathcal{S}^p(\mathcal{M})$ satisfies $\lambda(\beta_\lambda) = 1$ and $\lambda'(\beta_\lambda) = 0$ for all $\lambda \neq \lambda' \in \Lambda^p$. By definition of the local and global spaces and degrees of freedom, the global projector and the local projector fulfill, for any $Q \in \mathcal{Q}$,

$$(4.5) \quad (\Pi_{\mathcal{S}^p(\mathcal{M})}\varphi)|_Q = \Pi_{P_Q^p}(\varphi|_Q) = \sum_{\lambda_Q \in \Lambda_Q^p} \lambda_Q(\varphi|_Q)\beta_{\lambda_Q}.$$

For a given local functional $\lambda_Q(\cdot) = \lambda(\cdot|_Q)$ we have $\beta_{\lambda_Q} = \beta_\lambda|_Q$. Hence, the support of β_λ is given by all elements on which λ is defined, i.e., one element for all face point evaluations, two neighboring elements for all edge midpoint evaluations and, in case of vertex degrees of freedom, all elements around the vertex.

Corollary 4.7. *Let \mathcal{M} be a quadrilateral mesh of Ω , that fulfills the requirements of Section 2, with $h = \max_{Q \in \mathcal{Q}}(h_Q)$ and ρ from (2.6). Let $0 \leq \ell \leq 2$ and $4 \leq m \leq p+1$. There exists a constant $C > 0$, depending on ρ and p , such that we have for all $\varphi \in H^m(\Omega)$*

$$|\varphi - \Pi_{\mathcal{S}^p(\mathcal{M})}\varphi|_{H^\ell(\Omega)} \leq C h^{m-\ell} |\varphi|_{H^m(\Omega)},$$

as well as for $3 \leq m \leq p+1$, $3 \leq p$ and for all $\varphi \in W_\infty^m(\Omega)$

$$\|\varphi - \Pi_{\mathcal{S}^p(\mathcal{M})}\varphi\|_{L^\infty(\Omega)} \leq C h^m |\varphi|_{W_\infty^m(\Omega)}.$$

5. BASIS CONSTRUCTION, $p = 5$

In the following we describe how to compute the basis functions corresponding to one quadrilateral Q in the mesh. We define for every vertex six basis functions to interpolate the C^2 data, for every edge we define one basis function to interpolate the normal derivative at the edge midpoint. The remainder basis functions inside the element (with vanishing traces and derivatives on the element boundary) are selected to be standard Bernstein polynomials (for $p = 5$) or standard B-splines (for $p \in \{3, 4\}$). See [42, 45] for basics on B-splines.

To simplify the construction, we build a basis with respect to a slightly modified dual basis. Instead of point evaluations at the interior, we use integral-based functionals that are dual to the Bernstein polynomials (or B-splines).

Before we go into the details, we discuss the Bernstein-Bézier representation. Let \hat{b}_j be the Bernstein polynomials of degree 5, i.e., for $0 \leq j \leq 5$ and $\xi \in [0, 1]$,

$$\hat{b}_j(\xi) = \binom{5}{j} \xi^j (1-\xi)^{5-j}$$

and let $\hat{\mu}_i$ be the corresponding dual functionals, as in [21], i.e., $\hat{\mu}_i(\hat{b}_j) = \delta_i^j$. Let moreover

$$\mathbf{B} = \begin{pmatrix} \hat{b}_{0,5}(\xi_1, \xi_2) & & \hat{b}_{5,5}(\xi_1, \xi_2) \\ \vdots & \ddots & \vdots \\ \hat{b}_{0,0}(\xi_1, \xi_2) & \cdots & \hat{b}_{5,0}(\xi_1, \xi_2) \end{pmatrix} = \begin{pmatrix} \hat{b}_5(\xi_2) \\ \vdots \\ \hat{b}_0(\xi_2) \end{pmatrix} \begin{pmatrix} \hat{b}_0(\xi_1) & \cdots & \hat{b}_5(\xi_1) \end{pmatrix}$$

be the matrix of tensor-product Bernstein basis functions spanning $\mathbb{P}^{(5,5)}$.

For each basis function $\beta \in P_Q^5$, the pull-back $\widehat{\beta} = \beta \circ \mathbf{F}_Q$ possesses a biquintic tensor-product Bernstein-Bézier representation, having the coefficients $d_{j_1, j_2} \in \mathbb{R}$,

$$\widehat{\beta}(\xi_1, \xi_2) = \beta \circ \mathbf{F}_Q(\xi_1, \xi_2) = \sum_{j_1=0}^5 \sum_{j_2=0}^5 d_{j_1, j_2} \widehat{b}_{j_1, j_2}(\xi_1, \xi_2).$$

By means of a table of the form

$$\mathbf{D}[\beta] = \begin{array}{|c|c|c|c|} \hline d_{0,5} & d_{1,5} & \cdots & d_{5,5} \\ \hline \vdots & \vdots & & \vdots \\ \hline d_{0,1} & d_{1,1} & \cdots & d_{5,1} \\ \hline d_{0,0} & d_{1,0} & \cdots & d_{5,0} \\ \hline \end{array}$$

we can represent the basis function as $\widehat{\beta} = \mathbf{B} : \mathbf{D}[\beta]$, the Frobenius product of the matrix of basis functions with the coefficient matrix. Given the basis $b_{i_1, i_2} = \widehat{b}_{i_1, i_2} \circ \mathbf{F}_Q^{-1}$ we can define a dual basis μ_{j_1, j_2} as $\mu_{j_1, j_2}(\varphi) = \widehat{\mu}_{j_1} \otimes \widehat{\mu}_{j_2}(\varphi \circ \mathbf{F}_Q)$, satisfying $\mu_{j_1, j_2}(b_{i_1, i_2}) = \delta_{i_1}^{j_1} \delta_{i_2}^{j_2}$.

We now turn on defining the basis functions for P_Q^5 and dual functionals Λ_Q^5 . On each quadrilateral Q , we define 24 vertex basis functions (six for each vertex)

$$\mathbf{B}_{0,Q}^5 = \{\beta_{0,k,i}, \quad \text{for } k = 1, \dots, 4 \text{ and } i = 0, \dots, 5\},$$

determined by $\Lambda_{0,Q}$, four edge basis functions (one for each edge)

$$\mathbf{B}_{1,Q}^5 = \{\beta_{1,i}, \quad \text{for } i = 1, \dots, 4\},$$

determined by $\Lambda_{1,Q}^5$, and four patch-interior basis functions

$$\mathbf{B}_{2,Q}^5 = \{\beta_{2,i}, \quad \text{for } i = 1, \dots, 4\}.$$

To simplify the construction, we replace the point evaluation functionals $\Lambda_{2,Q}^5$ by the dual functionals of mapped tensor-product Bernstein polynomials

$$\mathbf{M}_{2,Q}^5 = \{\mu_{j_1, j_2}(\varphi) = \widehat{\mu}_{j_1} \otimes \widehat{\mu}_{j_2}(\varphi \circ \mathbf{F}_Q) : j_1, j_2 \in \{2, 3\}\}.$$

We define the basis

$$\mathbf{B}_Q^5 = \mathbf{B}_{0,Q}^5 \cup \mathbf{B}_{1,Q}^5 \cup \mathbf{B}_{2,Q}^5$$

in such a way that it is dual to

$$\mathbf{M}_Q^5 = \Lambda_{0,Q} \cup \Lambda_{1,Q} \cup \mathbf{M}_{2,Q}^5.$$

5.1. Patch interior basis functions. It is clear that we have, by definition,

$$\mathbf{B}_{2,Q}^5 = \{\beta_{2,1}, \beta_{2,2}, \beta_{2,3}, \beta_{2,4}\} = \{b_{2,2}, b_{2,3}, b_{3,2}, b_{3,3}\}.$$

In terms of their Bézier coefficients we have e.g.:

$$\mathbf{D}[b_{2,2}] = \begin{array}{|c|c|c|c|c|c|} \hline 0 & 0 & 0 & 0 & 0 & 0 \\ \hline 0 & 0 & 0 & 0 & 0 & 0 \\ \hline 0 & 0 & 0 & 0 & 0 & 0 \\ \hline 0 & 0 & 1 & 0 & 0 & 0 \\ \hline 0 & 0 & 0 & 0 & 0 & 0 \\ \hline 0 & 0 & 0 & 0 & 0 & 0 \\ \hline \end{array}$$

We trivially have $\text{span}(\mathbf{B}_{2,Q}^5) = \ker(\Lambda_{0,Q} \cup \Lambda_{1,Q})$.

5.2. Edge basis functions. We recall the notation introduced in Section 2: Let

$$\mathbf{t}^{(k)} = (t_1^{(k)}, t_2^{(k)})^T = \mathbf{v}_{k+1} - \mathbf{v}_k$$

be the vector corresponding to the edge ε_k and let $a^{(k)} = \det(\mathbf{t}^{(k-1)}, \mathbf{t}^{(k)})$. Then the edge basis function $\beta_{1,1}$, corresponding to edge ε_1 , is given by

$$\mathbf{D}[\beta_{1,1}] = \frac{8}{25\|\mathbf{t}^{(1)}\|} \begin{array}{|c|c|c|c|c|c|} \hline 0 & 0 & 0 & 0 & 0 & 0 \\ \hline 0 & 0 & 0 & 0 & 0 & 0 \\ \hline 0 & 0 & 0 & 0 & 0 & 0 \\ \hline 0 & 0 & 0 & 0 & 0 & 0 \\ \hline 0 & 0 & a^{(1)} & a^{(2)} & 0 & 0 \\ \hline 0 & 0 & 0 & 0 & 0 & 0 \\ \hline \end{array}$$

and analogously for $\beta_{1,2}$, $\beta_{1,3}$ and $\beta_{1,4}$. We have $\beta_{1,j} \in \ker(\Lambda_Q^0 \cup M_Q^2)$ and $\partial_{\mathbf{n}_{\varepsilon_i}} \beta_{1,j}(\mathbf{m}_{\varepsilon_i}) = \delta_i^j$, if the unit normal vector \mathbf{n}_i is assumed to point inwards.

5.3. Vertex basis functions. Before we define the coefficient matrices for the basis functions, we need to define some precomputable coefficients. We assume that all normal vectors point inwards and have

$$\mathbf{n}_{\varepsilon_k} = (n_1^{(k)}, n_2^{(k)})^T = \frac{1}{\|\mathbf{t}^{(k)}\|} (-t_2^{(k)}, t_1^{(k)})^T.$$

Let

$$\mathbf{q}^{(k)} = (q_1^{(k)}, q_2^{(k)})^T = \mathbf{v}_k - \mathbf{v}_{k+1} + \mathbf{v}_{k+2} - \mathbf{v}_{k+3}$$

and moreover

$$\begin{aligned} b_0^{(k)} &= \frac{\mathbf{t}^{(k-1)} \mathbf{t}^{(k)}}{\|\mathbf{t}^{(k)}\|^2}, \\ b_1^{(k)} &= \frac{\mathbf{t}^{(k+1)} \mathbf{t}^{(k)}}{\|\mathbf{t}^{(k)}\|^2}, \\ T_{i,j}^{(k)} &= t_i^{(k)} t_j^{(k)}, \\ Q_{i,j}^{(k)} &= t_i^{(k-1)} t_j^{(k)} + t_j^{(k-1)} t_i^{(k)}, \\ N_{i,j}^{(k)} &= n_i^{(k)} t_j^{(k)} + n_j^{(k)} t_i^{(k)}, \end{aligned}$$

for $i, j \in \{1, 2\}$ and $k \in \{1, 2, 3, 4\}$. Here k is considered modulo 4. We define

$$\mathbf{M}_k^L = \begin{array}{|c|c|c|c|c|c|} \hline 0 & 0 & 0 & 0 & 0 & 0 \\ \hline 0 & 0 & 0 & 0 & 0 & 0 \\ \hline 0 & -\frac{3}{5}b_0^{(k-1)} & 0 & 0 & 0 & 0 \\ \hline 1 & 1 + \frac{3}{5}b_1^{(k-1)} & 0 & 0 & 0 & 0 \\ \hline \frac{1}{2} & \frac{1}{2} & 0 & 0 & 0 & 0 \\ \hline 0 & 0 & 0 & 0 & 0 & 0 \\ \hline \end{array},$$

$$\mathbf{M}_k^B = \begin{array}{|c|c|c|c|c|c|} \hline 0 & 0 & 0 & 0 & 0 & 0 \\ \hline 0 & 0 & 0 & 0 & 0 & 0 \\ \hline 0 & 0 & 0 & 0 & 0 & 0 \\ \hline 0 & 0 & 0 & 0 & 0 & 0 \\ \hline 0 & \frac{1}{2} & 1 + \frac{3}{5}b_0^{(k)} & -\frac{3}{5}b_1^{(k)} & 0 & 0 \\ \hline 0 & \frac{1}{2} & 1 & 0 & 0 & 0 \\ \hline \end{array}$$

and

$$\mathbf{X} = \begin{array}{|c|c|c|c|c|c|} \hline 0 & 0 & 0 & 0 & 0 & 0 \\ \hline 0 & 0 & 0 & 0 & 0 & 0 \\ \hline 0 & 0 & 0 & 0 & 0 & 0 \\ \hline 0 & 0 & 0 & 0 & 0 & 0 \\ \hline \frac{1}{2} & 0 & 0 & 0 & 0 & 0 \\ \hline 1 & \frac{1}{2} & 0 & 0 & 0 & 0 \\ \hline \end{array}.$$

The vertex basis function $\beta_{0,1,0}$ is then given by

$$\mathbf{D}[\beta_{0,1,0}] = \mathbf{M}_1^L + \mathbf{M}_1^B + \mathbf{X}.$$

In general, the basis functions $\beta_{0,k,0}$ are given by

$$\mathbf{D}[\beta_{0,k,0}] = R_k(\mathbf{M}_k^L + \mathbf{M}_k^B + \mathbf{X})$$

where R_k is a suitable operator $R_k : \mathbb{R}^{6 \times 6} \rightarrow \mathbb{R}^{6 \times 6}$ taking care of the local reparametrization, rotating the positions of the vertices. Let

$$\mathbf{Y}_{k,i} = \begin{array}{|c|c|c|c|c|c|} \hline 0 & 0 & 0 & 0 & 0 & 0 \\ \hline 0 & 0 & 0 & 0 & 0 & 0 \\ \hline 0 & 0 & 0 & 0 & 0 & 0 \\ \hline 0 & -\frac{1}{5}t_i^{(k-2)} & 0 & 0 & 0 & 0 \\ \hline 0 & \frac{1}{10}q_i^{(k)} & \frac{1}{5}t_i^{(k+1)} & 0 & 0 & 0 \\ \hline 0 & 0 & 0 & 0 & 0 & 0 \\ \hline \end{array}$$

then the vertex basis functions $\beta_{0,k,1}$ and $\beta_{0,k,2}$ interpolating the derivatives in x_1 - and x_2 -direction, respectively, are given by

$$\begin{aligned} \mathbf{D}[\beta_{0,k,i}] &= \frac{2}{5}R_k \left(-t_i^{(k-1)}\mathbf{M}_k^L + t_i^{(k)}\mathbf{M}_k^B + \mathbf{Y}_{k,i} \right) \\ &\quad - \frac{5}{16}n_i^{(k)}\mathbf{D}[\beta_{1,k}] - \frac{5}{16}n_i^{(k-1)}\mathbf{D}[\beta_{1,k-1}], \end{aligned}$$

for $i = 1, 2$. Finally we define the vertex basis functions $\beta_{0,k,3}$, $\beta_{0,k,4}$ and $\beta_{0,k,5}$, interpolating the second derivatives. Let

$$\mathbf{Z}_{k,(i,j)} = \begin{array}{|c|c|c|c|c|c|} \hline 0 & 0 & 0 & 0 & 0 & 0 \\ \hline 0 & 0 & 0 & 0 & 0 & 0 \\ \hline 0 & 0 & 0 & 0 & 0 & 0 \\ \hline 0 & \frac{1}{5}Q_{i,j}^{(k-1)} & 0 & 0 & 0 & 0 \\ \hline -\frac{1}{2}T_{i,j}^{(k-1)} & -\frac{2}{5}Q_{i,j}^{(k)} - \frac{1}{2}T_{i,j}^{(k-1)} - \frac{1}{2}T_{i,j}^{(k)} & \frac{1}{5}Q_{i,j}^{(k+1)} & 0 & 0 & 0 \\ \hline 0 & -\frac{1}{2}T_{i,j}^{(k)} & 0 & 0 & 0 & 0 \\ \hline \end{array},$$

then we have

$$\begin{aligned} \mathbf{D}[\beta_{0,k,i+j+1}] &= \frac{\lambda}{20}R_k \left(T_{i,j}^{(k-1)}\mathbf{M}_k^L + T_{i,j}^{(k)}\mathbf{M}_k^B + \mathbf{Z}_{k,(i,j)} \right) \\ &\quad - \frac{\lambda}{32}N_{i,j}^{(k)}\mathbf{D}[\beta_{1,k}] + \frac{\lambda}{32}N_{i,j}^{(k-1)}\mathbf{D}[\beta_{1,k-1}] \end{aligned}$$

for $i, j \in \{1, 2\}$, where $\lambda = 2 - \delta_i^j$. All representations of basis functions are verifiable via symbolic computation, e.g. by using Mathematica. We have $\beta_{0,k,j} \in \ker(\Lambda_{1,Q} \cup M_{2,Q}^3)$ and

$$(\beta_{0,k,0}, \beta_{0,k,1}, \beta_{0,k,2}, \beta_{0,k,3}, \beta_{0,k,4}, \beta_{0,k,5})$$

being dual to

$$(\varphi(\mathbf{v}_k), \partial_1\varphi(\mathbf{v}_k), \partial_2\varphi(\mathbf{v}_k), \partial_1\partial_1\varphi(\mathbf{v}_k), \partial_1\partial_2\varphi(\mathbf{v}_k), \partial_2\partial_2\varphi(\mathbf{v}_k)),$$

with vanishing C^2 -data at all other vertices.

6. QUADRILATERAL MACRO-ELEMENT: DEFINITION AND BASIS CONSTRUCTION

We can extend the definition of polynomial BS quadrilaterals of degree $p \geq 5$ to certain B-spline based macro-elements of any degree $p \geq 3$. In that case the degrees of freedom are given as C^2 -data in the vertices, normal derivative and point data at certain points along the edges, as well as suitably many interior functions that have vanishing values and gradients at all element boundaries. In such a setting, refinement can be performed either by splitting the macro-elements or by knot insertion within every macro-element. Note that, in the construction below, the continuity within the macro-element is of order $p - 2$ for all degrees. In general, any order of continuity r , with $1 \leq r \leq p - 2$, can be achieved.

We assume that every quadrilateral Q is split into $k \times k$ elements by mapping a regular split of the parameter domain $\hat{Q} = [0, 1]^2$ using \mathbf{F}_Q . Let $\mathcal{S}_k^{p,r}$ be the univariate B-spline space of degree p and regularity r over the interval $[0, 1]$ split into k polynomial segments of the same length, i.e., having the knot vector

$$\left(0, \dots, 0, \frac{1}{k}, \frac{1}{k}, \frac{2}{k}, \frac{2}{k}, \dots, \frac{k-1}{k}, \frac{k-1}{k}, 1, \dots, 1\right)$$

for $r = p - 2$ and

$$\left(0, \dots, 0, \frac{1}{k}, \frac{2}{k}, \dots, \frac{k-1}{k}, 1, \dots, 1\right)$$

for $r = p - 1$, where the first and last knots are repeated $p + 1$ times. These knot vectors define piecewise polynomials on the split $s_k(\hat{Q})$ in the tensor-product case. Let θ_i^p , for $i = 0, \dots, 2k + p - 2$ and η_i^p , for $i = 0, \dots, k + p - 1$, be the corresponding Greville abscissae for the first and second knot vector, respectively. Note that the Greville abscissae γ_i corresponding to a given knot vector (ξ_0, \dots, ξ_N) are defined as knot averages $\gamma_i = (\xi_{i+1} + \dots + \xi_{i+p})/p$ for $i = 0, \dots, N - p - 1$.

As in Definition 3.2 we can define the local function space and the local degrees of freedom, where we need to assume $k \geq \max(1, 6 - p)$ in order to be able to split the vertex degrees of freedom.

Definition 6.1 (Local space and degrees of freedom). Given a quadrilateral Q with vertices $\mathbf{v}_1, \mathbf{v}_2, \mathbf{v}_3$ and \mathbf{v}_4 we define the C^1 quadrilateral spline macro-element of degree p as (Q, P_Q, Λ_Q) , with

$$P_Q = \left\{ \varphi : Q \rightarrow \mathbb{R}, \text{ with } \begin{array}{ll} (\varphi \circ \mathbf{F}_Q) & \in \mathcal{S}_k^{p,p-2} \otimes \mathcal{S}_k^{p,p-2}, \\ (\varphi \circ \mathbf{F}_Q)|_{\hat{\varepsilon}} & \in \mathcal{S}_k^{p,p-1}, \\ (\partial_{\mathbf{n}_{\hat{\varepsilon}}} \varphi \circ \mathbf{F}_Q)|_{\hat{\varepsilon}} & \in \mathcal{S}_k^{p-1,p-2}, \end{array} \text{ for each } \hat{\varepsilon} \text{ of } \hat{Q} \right\}$$

and

$$\begin{aligned} \Lambda_Q &= \Lambda_{0,Q} \cup \Lambda_{1,Q}^* \cup \Lambda_{2,Q}^*, \text{ with} \\ \Lambda_{0,Q} &= \{\varphi(\mathbf{v}_i), \partial_1 \varphi(\mathbf{v}_i), \partial_2 \varphi(\mathbf{v}_i), \partial_1 \partial_1 \varphi(\mathbf{v}_i), \partial_1 \partial_2 \varphi(\mathbf{v}_i), \partial_2 \partial_2 \varphi(\mathbf{v}_i), 1 \leq i \leq 4\}, \\ \Lambda_{1,Q}^* &= \{\varphi(r_{i,j_0}), \text{ for } 1 \leq i \leq 4, 1 \leq j_0 \leq k + p - 6\} \\ &\quad \cup \{\partial_{\mathbf{n}_{\hat{\varepsilon}_i}} \varphi(q_{i,j_1}), \text{ for } 1 \leq i \leq 4, 1 \leq j_1 \leq k + p - 5\}, \\ \Lambda_{2,Q}^* &= \{\varphi(\mathbf{x}), \mathbf{x} \in \mathcal{F}_Q^*\}. \end{aligned}$$

Here $r_{i,j_0} = \mathbf{F}_{\varepsilon_i}(\eta_{j_0+2}^p)$, $q_{i,j_1} = \mathbf{F}_{\varepsilon_i}(\eta_{j_1+1}^{p-1})$, with $\mathbf{F}_{\varepsilon_i} = \mathbf{F}_Q|_{\varepsilon_i}$, and the set of face points is given as

$$\mathcal{F}_Q^* = \{\mathbf{F}_Q(\theta_{j_1}^p, \theta_{j_2}^p), 2 \leq j_1, j_2 \leq 2k + p - 4\}.$$

We have the following.

Lemma 6.2. *Let (Q, P_Q, Λ_Q) be the element defined in Definition 6.1. The degrees of freedom Λ_Q completely determine the space P_Q .*

Proof. This lemma is a direct consequence of the results developed in [26, Section 4]. For the sake of completeness, we present the main steps of the proof in the following. Let $\widehat{\varphi} = \varphi \circ \mathbf{F}_Q$. Let us consider the conditions on φ (and consequently on $\widehat{\varphi}$) along one edge ε , w.l.o.g. $\varepsilon = \{0\} \times]0, 1[$. For the unit normal vector \mathbf{n} along ε , we then have

$$\mathbf{n} = \lambda(\xi_2)\partial_1\mathbf{F}_Q(0, \xi_2) + \mu(\xi_2)\partial_2\mathbf{F}_Q(0, \xi_2) = \lambda(\xi_2)\mathbf{v}(\xi_2) - \mu(\xi_2)\mathbf{t}^{(4)},$$

with $\mathbf{v}(\xi_2) = \mathbf{t}^{(1)}(1 - \xi_2) - \mathbf{t}^{(3)}\xi_2$, where

$$\lambda(\xi_2) = \frac{\|\mathbf{t}^{(4)}\|}{\det(\mathbf{v}(\xi_2), \mathbf{t}^{(4)})} = \frac{1}{\alpha(\xi_2)} \quad \text{and} \quad \mu(\xi_2) = \frac{\mathbf{v}(\xi_2) \cdot \mathbf{t}^{(4)}}{\det(\mathbf{v}(\xi_2), \mathbf{t}^{(4)})\|\mathbf{t}^{(4)}\|} = \frac{\beta(\xi_2)}{\alpha(\xi_2)}.$$

It is easy to check, that $\mathbf{n} \cdot \mathbf{t}^{(4)} = 0$ and

$$\mathbf{n} \cdot \mathbf{n} = \frac{1}{\det(\mathbf{v}(\xi_2), \mathbf{t}^{(4)})^2} \left(\|\mathbf{v}(\xi_2)\|^2 \|\mathbf{t}^{(4)}\|^2 - (\mathbf{v}(\xi_2) \cdot \mathbf{t}^{(4)})^2 \right) = 1.$$

Then, the chain rule yields

$$(\partial_{\mathbf{n}}\varphi \circ \mathbf{F}_Q)|_{\varepsilon} = \nabla\widehat{\varphi}(\nabla\mathbf{F}_Q)^{-1} \cdot \mathbf{n}|_{\varepsilon} = \lambda(\xi_2)\partial_1\widehat{\varphi}(0, \xi_2) + \mu(\xi_2)\partial_2\widehat{\varphi}(0, \xi_2).$$

Let $f_0 = \widehat{\varphi}|_{\varepsilon} \in \mathcal{S}_k^{p,p-1}$ and $f_1 = (\partial_{\mathbf{n}}\varphi \circ \mathbf{F}_Q)|_{\varepsilon} \in \mathcal{S}_k^{p-1,p-2}$. Then

$$\widehat{\varphi}(0, \xi_2) = f_0(\xi_2)$$

and

$$\partial_1\widehat{\varphi}(0, \xi_2) = \alpha(\xi_2)f_1(\xi_2) - \beta(\xi_2)f_0'(\xi_2) \in \mathcal{S}_k^{p,p-2},$$

since $\alpha(\xi_2)$ and $\beta(\xi_2)$ are linear functions.

The trace $f_0 \in \mathcal{S}_k^{p,p-1}$, with $\dim(\mathcal{S}_k^{p,p-1}) = k + p$, is completely determined by the C^2 -data at the vertices (3 degrees of freedom at each vertex) together with the $k + p - 6$ point evaluations $\varphi(r_{i,j_0})$, since the points are selected as suitable mapped Greville points. Similarly, the normal derivative along an edge $f_1 \in \mathcal{S}_k^{p-1,p-2}$, a spline space of dimension $k + p - 1$, is completely determined by the C^2 -data at the vertices (determining 2 degrees of freedom each) as well as by the $k + p - 5$ normal derivative evaluations at Greville points, i.e., $\partial_{\mathbf{n}_{\varepsilon_i}}\varphi(q_{i,j_1})$. The space $\mathcal{S}_k^{p,p-2} \otimes \mathcal{S}_k^{p,p-2}$ has a standard tensor-product basis $\{\hat{b}_{i_1}(\xi_1)\hat{b}_{i_2}(\xi_2), 0 \leq i_1, i_2 \leq 2k + p - 2\}$. Hence, every function $\widehat{\varphi} \in \mathcal{S}_k^{p,p-2} \otimes \mathcal{S}_k^{p,p-2}$ is represented by coefficients c_{i_1, i_2} , such that

$$\widehat{\varphi}(\xi_1, \xi_2) = \sum_{i_1=0}^{n-1} \sum_{i_2=0}^{n-1} c_{i_1, i_2} \hat{b}_{i_1}(\xi_1) \hat{b}_{i_2}(\xi_2).$$

with $n = 2k + p - 1$. All coefficients c_{0, i_2}, c_{1, i_2} , for $0 \leq i_2 \leq n$, are determined by f_0 and f_1 . Analogously, the coefficients $c_{n-1, i_2}, c_{n-2, i_2}, c_{i_1, 0}, c_{i_1, 1}, c_{i_1, n-1}$ and $c_{i_1, n-2}$ corresponding to the remaining edges are also determined by $\Lambda_{0, Q}$ and $\Lambda_{1, Q}^*$. All remaining coefficients c_{i_1, i_2} , for $2 \leq i_1, i_2 \leq n - 3$, corresponding to the space

$$\{\widehat{\varphi} \in \mathcal{S}_k^{p,p-2} \otimes \mathcal{S}_k^{p,p-2} : \widehat{\varphi}|_{\partial\widehat{\Omega}} = 0, \nabla\widehat{\varphi}|_{\partial\widehat{\Omega}} = \mathbf{0}\}$$

are determined by the $(n-4)^2$ evaluations at mapped Greville points $\mathbf{F}_Q(\theta_{j_1}^p, \theta_{j_2}^p)$. Consequently, the full space P_Q is completely determined by the dual functionals Λ_Q and the proof is complete. \square

It follows immediately from Lemma 6.2 that the dimension of the space can be determined completely by counting, having six degrees of freedom per vertex, $2k+2p-11$ degrees of freedom per edge and $(2k+p-5)^2$ degrees of freedom inside the element. Thus, we need $2k+2p-11 \geq 0$, yielding the constraint $k \geq 6-p$.

In the remainder of this section, we present in more detail the two special cases of C^1 quadrilateral macro-elements presented in Definition 3.6. Since we need $k \geq \max(1, 6-p)$, they represent the spline elements with the least number of inner knots, allowing a separation of degrees of freedom at the vertices. For $p=4$ we consider the spline space with one inner knot at $\frac{1}{2}$ with multiplicity two in each direction $\mathcal{S}_2^{4,2} \otimes \mathcal{S}_2^{4,2}$, having the basis \hat{b}_{j_1, j_2}^4 and corresponding dual basis $\hat{\mu}_{j_1, j_2}^4$ for $0 \leq j_1, j_2 \leq 6$. For $p=3$ we consider the spline space $\mathcal{S}_3^{3,1} \otimes \mathcal{S}_3^{3,1}$, with basis \hat{b}_{j_1, j_2}^3 and dual basis $\hat{\mu}_{j_1, j_2}^3$ for $0 \leq j_1, j_2 \leq 7$, see [42, 45].

Hence, for smaller degrees that patches Q are macro-elements with 2×2 (for $p=4$) or 3×3 (for $p=3$) polynomial sub-elements. Let $n = 11 - p$. We write, as for $p=5$, all tensor-product basis functions in a matrix

$$\mathbf{B} = \begin{pmatrix} \hat{b}_{0, n-1}^p & \cdots & \hat{b}_{n-1, n-1}^p \\ \vdots & & \vdots \\ \hat{b}_{0, 0}^p & \cdots & \hat{b}_{n-1, 0}^p \end{pmatrix}$$

and denote again with $\mathbf{D}[\beta]$ the $(n \times n)$ -matrix of coefficients. As for $p=5$, let $b_{j_1, j_2}^p = \hat{b}_{j_1, j_2}^p \circ \mathbf{F}_Q^{-1}$ denote the basis functions on the element Q .

6.1. Patch interior basis functions. We have $(n-4)^2$ basis functions

$$B_{2, Q}^p = \{b_{j_1, j_2}^p, 2 \leq j_1, j_2 \leq n-3\},$$

which satisfy $\text{span}(B_{2, Q}^p) = \ker(\Lambda_{0, Q} \cup \Lambda_{1, Q})$.

6.2. Edge basis functions. The edge basis function $\beta_{1,1}$, corresponding to edge ε_1 , is given for $p=4$ by

$$\mathbf{D}[\beta_{1,1}] = \frac{1}{32 \|\mathbf{t}^{(1)}\|} \begin{array}{|c|c|c|c|c|c|c|} \hline 0 & 0 & 0 & 0 & 0 & 0 & 0 \\ \hline 0 & 0 & 0 & 0 & 0 & 0 & 0 \\ \hline 0 & 0 & 0 & 0 & 0 & 0 & 0 \\ \hline 0 & 0 & 0 & 0 & 0 & 0 & 0 \\ \hline 0 & 0 & 0 & 0 & 0 & 0 & 0 \\ \hline 0 & 0 & 2a^{(1)} & 3a^{(1)} + 3a^{(2)} & 2a^{(2)} & 0 & 0 \\ \hline 0 & 0 & 0 & 0 & 0 & 0 & 0 \\ \hline \end{array},$$

and for $p = 3$ by

$$\mathbf{D}[\beta_{1,1}] = \frac{2}{81\|\mathbf{t}^{(1)}\|} \begin{array}{|c|c|c|c|c|c|c|c|} \hline 0 & 0 & 0 & 0 & 0 & 0 & 0 & 0 \\ \hline 0 & 0 & 0 & 0 & 0 & 0 & 0 & 0 \\ \hline 0 & 0 & 0 & 0 & 0 & 0 & 0 & 0 \\ \hline 0 & 0 & 0 & 0 & 0 & 0 & 0 & 0 \\ \hline 0 & 0 & 0 & 0 & 0 & 0 & 0 & 0 \\ \hline 0 & 0 & 0 & 0 & 0 & 0 & 0 & 0 \\ \hline 0 & 0 & a^{(1)} & 3a^{(1)} + 2a^{(2)} & 2a^{(1)} + 3a^{(2)} & a^{(2)} & 0 & 0 \\ \hline 0 & 0 & 0 & 0 & 0 & 0 & 0 & 0 \\ \hline \end{array}.$$

The functions $\beta_{1,2}$, $\beta_{1,3}$ and $\beta_{1,4}$ are defined analogously. Analogously to the polynomial case, we have $\beta_{1,j} \in \ker(\Lambda_{0,Q} \cup M_{2,Q}^p)$ and $\partial_{\mathbf{n}_{\varepsilon_i}} \beta_{1,j}(\mathbf{m}_{\varepsilon_i}) = \delta_i^j$, if the unit normal vector \mathbf{n}_i is assumed to point inwards.

6.3. Vertex basis functions, $p = 4$. We define

$$\mathbf{M}_k^L = \begin{array}{|c|c|c|c|c|c|c|c|} \hline 0 & 0 & 0 & 0 & 0 & 0 & 0 & 0 \\ \hline 0 & 0 & 0 & 0 & 0 & 0 & 0 & 0 \\ \hline 0 & -\frac{1}{8}b_0^{(k-1)} & 0 & 0 & 0 & 0 & 0 & 0 \\ \hline \frac{1}{2} & \frac{1}{2} + \frac{3}{16}(b_1^{(k-1)} - b_0^{(k-1)}) & 0 & 0 & 0 & 0 & 0 & 0 \\ \hline \frac{2}{3} & \frac{2}{3} + \frac{1}{8}b_1^{(k-1)} & 0 & 0 & 0 & 0 & 0 & 0 \\ \hline \frac{1}{3} & \frac{1}{3} & 0 & 0 & 0 & 0 & 0 & 0 \\ \hline 0 & 0 & 0 & 0 & 0 & 0 & 0 & 0 \\ \hline \end{array},$$

$$\mathbf{M}_k^B = \begin{array}{|c|c|c|c|c|c|c|c|} \hline 0 & 0 & 0 & 0 & 0 & 0 & 0 & 0 \\ \hline 0 & 0 & 0 & 0 & 0 & 0 & 0 & 0 \\ \hline 0 & 0 & 0 & 0 & 0 & 0 & 0 & 0 \\ \hline 0 & 0 & 0 & 0 & 0 & 0 & 0 & 0 \\ \hline 0 & 0 & 0 & 0 & 0 & 0 & 0 & 0 \\ \hline 0 & \frac{1}{3} & \frac{2}{3} + \frac{1}{8}b_0^{(k)} & \frac{1}{2} + \frac{3}{16}(b_0^{(k)} - b_1^{(k)}) & -\frac{1}{8}b_1^{(k)} & 0 & 0 & 0 \\ \hline 0 & \frac{1}{3} & \frac{2}{3} & \frac{1}{2} & 0 & 0 & 0 & 0 \\ \hline \end{array}$$

and

$$\mathbf{X} = \begin{array}{|c|c|c|c|c|c|c|c|} \hline 0 & 0 & 0 & 0 & 0 & 0 & 0 & 0 \\ \hline 0 & 0 & 0 & 0 & 0 & 0 & 0 & 0 \\ \hline 0 & 0 & 0 & 0 & 0 & 0 & 0 & 0 \\ \hline 0 & 0 & 0 & 0 & 0 & 0 & 0 & 0 \\ \hline \frac{1}{3} & \frac{1}{3} & 0 & 0 & 0 & 0 & 0 & 0 \\ \hline \frac{2}{3} & \frac{1}{3} & \frac{1}{3} & 0 & 0 & 0 & 0 & 0 \\ \hline 1 & \frac{2}{3} & \frac{1}{3} & 0 & 0 & 0 & 0 & 0 \\ \hline \end{array}.$$

The basis functions $\beta_{0,k,0}$ are given by

$$\mathbf{D}[\beta_{0,k,0}] = R_k(\mathbf{M}_k^L + \mathbf{M}_k^B + \mathbf{X}).$$

Let

$$\mathbf{Y}_{k,i} = \begin{array}{|c|c|c|c|c|c|c|} \hline 0 & 0 & 0 & 0 & 0 & 0 & 0 \\ \hline 0 & 0 & 0 & 0 & 0 & 0 & 0 \\ \hline 0 & 0 & 0 & 0 & 0 & 0 & 0 \\ \hline 0 & -\frac{1}{24}t_i^{(k-2)} & 0 & 0 & 0 & 0 & 0 \\ \hline 0 & -\frac{1}{4}t_i^{(k-2)} - \frac{1}{6}q_i^{(k)} & 0 & 0 & 0 & 0 & 0 \\ \hline 0 & \frac{1}{24}q_i^{(k)} & \frac{1}{4}t_i^{(k+1)} - \frac{1}{6}q_i^{(k)} & \frac{1}{24}t_i^{(k+1)} & 0 & 0 & 0 \\ \hline 0 & 0 & 0 & 0 & 0 & 0 & 0 \\ \hline \end{array},$$

then the vertex basis functions $\beta_{0,k,1}$ and $\beta_{0,k,2}$ are given by

$$\mathbf{D}[\beta_{0,k,i}] = \frac{3}{8}R_k \left(-t_i^{(k-1)}\mathbf{M}_k^L + t_i^{(k)}\mathbf{M}_k^B + \mathbf{Y}_{k,i} \right) - \frac{1}{4}n_i^{(k)}\mathbf{D}[\beta_{1,k}] - \frac{1}{4}n_i^{(k-1)}\mathbf{D}[\beta_{1,k-1}],$$

for $i = 1, 2$. Let

$$\mathbf{Z}_{k,(i,j)} = \begin{array}{|c|c|c|c|c|c|} \hline 0 & 0 & 0 & 0 & 0 & \dots \\ \hline 0 & 0 & 0 & 0 & 0 & \\ \hline 0 & 0 & 0 & 0 & 0 & \\ \hline 0 & \frac{1}{32}Q_{i,j}^{(k-1)} & 0 & 0 & 0 & \\ \hline -\frac{1}{6}T_{i,j}^{(k-1)} & -\frac{1}{6}T_{i,j}^{(k-1)} & 0 & 0 & 0 & \\ \hline & -\frac{1}{8}Q_{i,j}^{(k)} + \frac{1}{16}Q_{i,j}^{(k-1)} & & & & \\ \hline -\frac{1}{3}T_{i,j}^{(k-1)} & -\frac{1}{3}T_{i,j}^{(k-1)} & -\frac{1}{8}Q_{i,j}^{(k)} + \frac{1}{16}Q_{i,j}^{(k+1)} & \frac{1}{32}Q_{i,j}^{(k+1)} & 0 & \\ \hline & -\frac{1}{3}T_{i,j}^{(k)} - \frac{3}{16}Q_{i,j}^{(k)} & -\frac{1}{6}T_{i,j}^{(k)} & & & \\ \hline 0 & -\frac{1}{3}T_{i,j}^{(k)} & -\frac{1}{6}T_{i,j}^{(k)} & 0 & 0 & \dots \\ \hline \end{array},$$

then we have

$$\mathbf{D}[\beta_{0,k,i+j+1}] = \frac{\lambda}{24}R_k \left(T_{i,j}^{(k-1)}\mathbf{M}_k^L + T_{i,j}^{(k)}\mathbf{M}_k^B + \mathbf{Z}_{k,(i,j)} \right) - \frac{\lambda}{48}N_{i,j}^{(k)}\mathbf{D}[\beta_{1,k}] + \frac{\lambda}{48}N_{i,j}^{(k-1)}\mathbf{D}[\beta_{1,k-1}]$$

for $i, j \in \{1, 2\}$, where $\lambda = 2 - \delta_i^j$. We have $\beta_{0,k,j} \in \ker(\Lambda_{1,Q} \cup M_{2,Q}^4)$ and $\{\beta_{0,k,j}\}_{k=1,\dots,4,j=0,\dots,5}$ being dual to $\Lambda_{0,Q}$.

6.4. Vertex basis functions, $p = 3$. We define

$$\mathbf{M}_k^L = \begin{array}{|c|c|c|c|c|c|c|c|} \hline 0 & 0 & 0 & 0 & 0 & 0 & 0 & 0 \\ \hline 0 & 0 & 0 & 0 & 0 & 0 & 0 & 0 \\ \hline 0 & -\frac{1}{18}b_0^{(k-1)} & 0 & 0 & 0 & 0 & 0 & 0 \\ \hline \frac{1}{3} & \frac{1}{3} + \frac{1}{9}b_1^{(k-1)} - \frac{1}{6}b_0^{(k-1)} & 0 & 0 & 0 & 0 & 0 & 0 \\ \hline \frac{2}{3} & \frac{2}{3} + \frac{1}{6}b_1^{(k-1)} - \frac{1}{9}b_0^{(k-1)} & 0 & 0 & 0 & 0 & 0 & 0 \\ \hline \frac{2}{3} & \frac{2}{3} + \frac{1}{18}b_1^{(k-1)} & 0 & 0 & 0 & 0 & 0 & 0 \\ \hline \frac{1}{3} & \frac{1}{3} & 0 & 0 & 0 & 0 & 0 & 0 \\ \hline 0 & 0 & 0 & 0 & 0 & 0 & 0 & 0 \\ \hline \end{array},$$

$$\mathbf{M}_k^B =$$

0	0	0	0	0	0	0	0
0	0	0	0	0	0	0	0
0	0	0	0	0	0	0	0
0	0	0	0	0	0	0	0
0	0	0	0	0	0	0	0
0	0	0	0	0	0	0	0
0	$\frac{1}{3}$	$\frac{2}{3} + \frac{1}{18}b_0^{(k)}$	$\frac{2}{3} + \frac{1}{6}b_0^{(k)} - \frac{1}{9}b_1^{(k)}$	$\frac{1}{3} + \frac{1}{9}b_0^{(k)} - \frac{1}{6}b_1^{(k)}$	$-\frac{1}{18}b_1^{(k)}$	0	0
0	$\frac{1}{3}$	$\frac{2}{3}$	$\frac{2}{3}$	$\frac{1}{3}$	0	0	0

and

$$\mathbf{X} = \begin{array}{c} \begin{array}{|c|c|c|c|c|c|c|c|} \hline 0 & 0 & 0 & 0 & 0 & 0 & 0 & 0 \\ \hline 0 & 0 & 0 & 0 & 0 & 0 & 0 & 0 \\ \hline 0 & 0 & 0 & 0 & 0 & 0 & 0 & 0 \\ \hline 0 & 0 & 0 & 0 & 0 & 0 & 0 & 0 \\ \hline 0 & 0 & 0 & 0 & 0 & 0 & 0 & 0 \\ \hline \frac{1}{3} & \frac{1}{3} & 0 & 0 & 0 & 0 & 0 & 0 \\ \hline \frac{2}{3} & \frac{1}{3} & \frac{1}{3} & 0 & 0 & 0 & 0 & 0 \\ \hline 1 & \frac{2}{3} & \frac{1}{3} & 0 & 0 & 0 & 0 & 0 \\ \hline \end{array} \\ \cdot \end{array}.$$

The basis functions $\beta_{0,k,0}$ are given by

$$\mathbf{D}[\beta_{0,k,0}] = R_k(\mathbf{M}_k^L + \mathbf{M}_k^B + \mathbf{X}).$$

Let

$$\mathbf{Y}_{k,i} =$$

0	0	0	0	0	0	0	0
0	0	0	0	0	0	0	0
0	0	0	0	0	0	0	0
0	0	0	0	0	0	0	0
0	$-\frac{1}{18}t_i^{(k-2)} - \frac{1}{54}q_i^{(k)}$	0	0	0	0	0	0
0	$-\frac{5}{18}t_i^{(k-2)} - \frac{11}{54}q_i^{(k)}$	0	0	0	0	0	0
0	$\frac{1}{27}q_i^{(k)}$	$\frac{5}{18}t_i^{(k+1)} - \frac{11}{54}q_i^{(k)}$	$\frac{1}{18}t_i^{(k+1)} - \frac{1}{54}q_i^{(k)}$	0	0	0	0
0	0	0	0	0	0	0	0

then the vertex basis functions $\beta_{0,k,1}$ and $\beta_{0,k,2}$ are given by

$$\begin{aligned} \mathbf{D}[\beta_{0,k,i}] &= \frac{1}{3}R_k \left(-t_i^{(k-1)}\mathbf{M}_k^L + t_i^{(k)}\mathbf{M}_k^B + \mathbf{Y}_{k,i} \right) \\ &\quad - \frac{1}{8}n_i^{(k)}\mathbf{D}[\beta_{1,k}] - \frac{1}{8}n_i^{(k-1)}\mathbf{D}[\beta_{1,k-1}], \end{aligned}$$

for $i = 1, 2$. Let

$$\mathbf{Z}_{k,(i,j)} = \begin{array}{c} \begin{array}{|c|c|c|c|c|c|} \hline 0 & 0 & 0 & 0 & 0 & \dots \\ \hline 0 & 0 & 0 & 0 & 0 & \\ \hline 0 & 0 & 0 & 0 & 0 & \\ \hline 0 & 0 & 0 & 0 & 0 & \\ \hline 0 & -\frac{1}{72}Q_{i,j}^{(k)} + \frac{1}{36}Q_{i,j}^{(k-1)} & 0 & 0 & 0 & \\ \hline -\frac{1}{6}T_{i,j}^{(k-1)} & -\frac{1}{6}T_{i,j}^{(k-1)} & 0 & 0 & 0 & \\ \hline & -\frac{11}{72}Q_{i,j}^{(k)} + \frac{1}{18}Q_{i,j}^{(k-1)} & & & & \\ \hline -\frac{1}{3}T_{i,j}^{(k-1)} & -\frac{1}{3}T_{i,j}^{(k-1)} & -\frac{11}{72}Q_{i,j}^{(k)} + \frac{1}{18}Q_{i,j}^{(k+1)} & \frac{1}{36}Q_{i,j}^{(k+1)} & 0 & \\ \hline & -\frac{1}{3}T_{i,j}^{(k)} - \frac{1}{6}Q_{i,j}^{(k)} & -\frac{1}{6}T_{i,j}^{(k)} & -\frac{1}{72}Q_{i,j}^{(k)} & & \\ \hline 0 & -\frac{1}{3}T_{i,j}^{(k)} & -\frac{1}{6}T_{i,j}^{(k)} & 0 & 0 & \dots \\ \hline \end{array} , \end{array}$$

then we have

$$\begin{aligned} \mathbf{D}[\beta_{0,k,i+j+1}] &= \frac{\lambda}{27}R_k \left(T_{i,j}^{(k-1)}\mathbf{M}_k^L + T_{i,j}^{(k)}\mathbf{M}_k^B + \mathbf{Z}_{k,(i,j)} \right) \\ &\quad - \frac{\lambda}{96}N_{i,j}^{(k)}\mathbf{D}[\beta_{1,k}] + \frac{\lambda}{96}N_{i,j}^{(k-1)}\mathbf{D}[\beta_{1,k-1}] \end{aligned}$$

for $i, j \in \{1, 2\}$, where $\lambda = 2 - \delta_i^j$. We have $\beta_{0,k,j} \in \ker(\Lambda_{1,Q} \cup \mathbf{M}_{2,Q}^3)$ and $\{\beta_{0,k,j}\}_{k=1,\dots,4,j=0,\dots,5}$ being dual to $\Lambda_{0,Q}$.

As for $p = 5$, all representations of basis functions for $p \in \{3, 4\}$ can be verified using simple symbolic computations.

7. EXTENSION TO ISOPARAMETRIC/ISOGEOMETRIC ELEMENTS

As pointed out before, the BS quadrilaterals and related spline macro-elements are not affine invariant. Hence their definition depends on the underlying geometry. It is possible to extend the construction from bilinearly mapped quadrilaterals Q , with $\mathbf{F}_Q \in (\mathbb{P}^{(1,1)})^2$, to fully isoparametric elements, with $\mathbf{F}_Q \in (P_Q^p)^2$. This naturally leads to the C^1 multi-patch isogeometric space proposed in [25], which is based on the previous works [27, 13, 23, 24]. The isoparametric/isogeometric extension, however, needs some additional care, in order to guarantee optimal approximation properties. First, the definition of the space P_Q^p and the associated degrees of freedom need to be generalized, mainly replacing the normal derivative $(\partial_{\mathbf{n}_\varepsilon} \varphi \circ \mathbf{F}_Q)|_\varepsilon$ with a suitable directional derivative $(\mathbf{d} \cdot \nabla \varphi \circ \mathbf{F}_Q)|_\varepsilon$ (in the bilinear case, \mathbf{d} is a constant normal vector which is then rescaled to the unitary normal \mathbf{n}). Secondly, and most importantly, the element parametrizations need to fulfill a condition (named analysis-suitable G^1 in the papers mentioned above) that holds for all bilinear parametrizations but requires a suitable refitting for higher degree parametrizations, see [24].

Modifications of elements near curved boundaries were also discussed and resolved successfully in [4] for a C^1 space of degree 4 and 5 over a quadrilateral mesh. There, the authors presented the construction of a minimal determining set (similar to a dual basis), without giving explicit degrees of freedom or a basis representation.

A complete analysis of the convergence in case of local modifications near the boundary is not known and beyond the scope of the current paper. It is important to note, that a suitable splitting of elements can increase the flexibility of the resulting space, such as in [19], where using a regular 4-split on degree $p = 5$ triangular elements allows for the construction of surfaces of arbitrary topology.

8. NUMERICAL EXAMPLES

The goal is to demonstrate the potential of using the proposed C^1 spaces over quadrilateral meshes \mathcal{M} for solving fourth order PDEs over domains Ω with piecewise linear boundary. This is done on the basis of a particular example, namely for the biharmonic equation

$$(8.1) \quad \begin{cases} \Delta^2 u(\mathbf{x}) = g(\mathbf{x}) & \mathbf{x} \in \Omega \\ u(\mathbf{x}) = g_1(\mathbf{x}) & \mathbf{x} \in \partial\Omega \\ \frac{\partial u}{\partial \mathbf{n}}(\mathbf{x}) = g_2(\mathbf{x}) & \mathbf{x} \in \partial\Omega. \end{cases}$$

More precisely, we solve problem (8.1) via a standard Galerkin discretization by employing the family of C^1 quadrilateral spaces $\mathcal{S}^p(\mathcal{M}_h)$, where the mesh size h denotes the length of the longest edge in \mathcal{M}_h , with $h = h_0 \frac{1}{2^L}$, $L = 0, 1, \dots, 5$. Here L denotes the level of refinement, h_0 is the mesh size of the initial mesh \mathcal{M} , and $\mathcal{M}_h = (\mathcal{Q}_h, \mathcal{E}_h, \mathcal{V}_h)$ is the resulting refined quadrilateral mesh obtained from \mathcal{M} with corresponding sets of quadrilaterals \mathcal{Q}_h , edges \mathcal{E}_h and vertices \mathcal{V}_h . Note that in the refinement process, each quadrilateral of the current mesh is split regularly into four sub-quadrilaterals. Moreover, in all examples below, the functions g , g_1 and g_2 from problem (8.1) are computed from an exact solution u , and the resulting Dirichlet boundary data g_1 and g_2 are L^2 projected and strongly imposed to the numerical solution $u_h \in \mathcal{S}^p(\mathcal{M}_h)$.

Example 8.1. For the two meshes \mathcal{M} in Fig. 5 and Fig. 6, which are visualized in the top left of each figure, we solve the biharmonic equation (8.1) over the corresponding bilinear multi-patch domains by using the BS quadrilateral and macro-element spaces $\mathcal{S}^p(\mathcal{M}_h)$ for polynomial degrees $p = 3, 4, 5$. For both cases, the considered exact solution is given by

$$(8.2) \quad u(x_1, x_2) = -4 \cos\left(\frac{x_1}{2}\right) \sin\left(\frac{x_2}{2}\right),$$

and is shown in Fig. 5 (top row, right) and Fig. 6 (top row, right), respectively. The resulting L^∞ -error as well as the relative L^2 , H^1 and H^2 -errors with respect to the number of degrees of freedom (NDOF) are shown in the middle and bottom rows of Fig. 5 and Fig. 6, and decrease for both examples with optimal order of $\mathcal{O}(h^{p+1})$, $\mathcal{O}(h^{p+1})$, $\mathcal{O}(h^p)$ and $\mathcal{O}(h^{p-1})$, respectively.

Example 8.2. We compare the C^1 quadrilateral spaces $\mathcal{S}^p(\mathcal{M}_h)$ for polynomial degrees $p = 3, 4, 5$ as constructed in this paper with the C^1 isogeometric spaces \mathcal{A}_h for the cases $(p, r) = (3, 1)$, $(p, r) = (4, 2)$ and $(p, r) = (5, 3)$ as generated in [26] by means of standard h -refinement. For this purpose, we solve the biharmonic equation (8.1) for the exact solution

$$(8.3) \quad u(x_1, x_2) = -4 \cos\left(\frac{x_1}{2}\right) \sin\left(\frac{x_2}{2}\right),$$

see Fig. 7 (top row, right), on the bilinearly parametrized multi-patch domain Ω determined by the mesh \mathcal{M} shown in Fig. 7 (top row, left). The resulting L^∞ -error as well as the relative L^2 , H^1 and H^2 -errors, which are reported in Fig. 7 (middle and bottom row) with respect to the number of degrees of freedom (NDOF), indicate for all considered degrees $p = 3, 4, 5$ and for both spaces $\mathcal{S}^p(\mathcal{M}_h)$ and \mathcal{A}_h convergence rates of optimal order of $\mathcal{O}(h^{p+1})$, $\mathcal{O}(h^{p+1})$, $\mathcal{O}(h^p)$ and $\mathcal{O}(h^{p-1})$, respectively. While the spaces $\mathcal{S}^p(\mathcal{M}_h)$ perform slightly better than the spaces \mathcal{A}_h

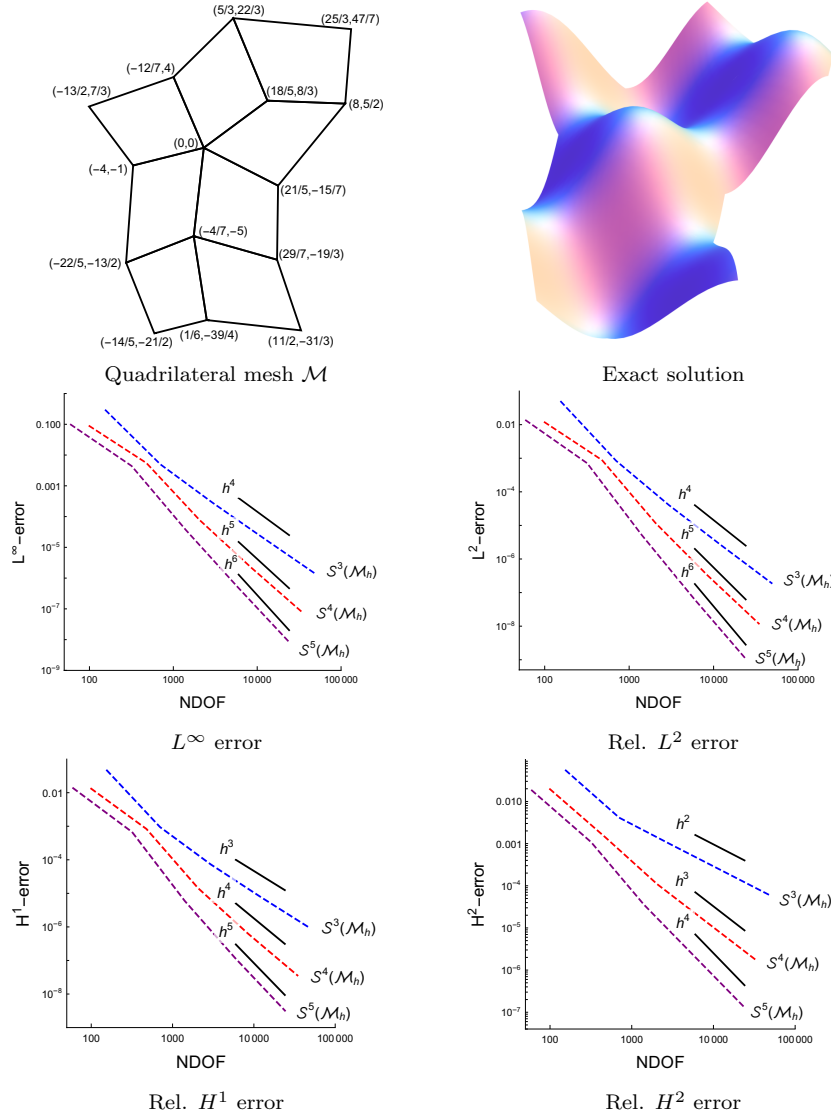


FIGURE 5. Solving the biharmonic equation (8.1) on the given quadrilateral mesh \mathcal{M} (top row, left) for the exact solution (8.2) (top row, right) with the resulting L^∞ and relative L^2 , H^1 , H^2 -errors (middle and bottom row). See Example 8.1.

for the case $p = 3$, it is in the opposite way around for the case $p = 5$. This is not really surprising, since for the case $p = 3$, the resulting spaces $\mathcal{S}^p(\mathcal{M}_h)$ are C^2 at all vertices $\mathbf{v} \in \mathcal{V}_h$, while the spaces \mathcal{A}_h are in general just C^1 at the vertices $\mathbf{v} \in \mathcal{V}_h \setminus \mathcal{V}$, and since for the case $p = 5$, e.g., the spaces \mathcal{A}_h are C^3 at all edges $\varepsilon \in \mathcal{E}_h$, while the spaces $\mathcal{S}^p(\mathcal{M}_h)$ are in general just C^1 there.

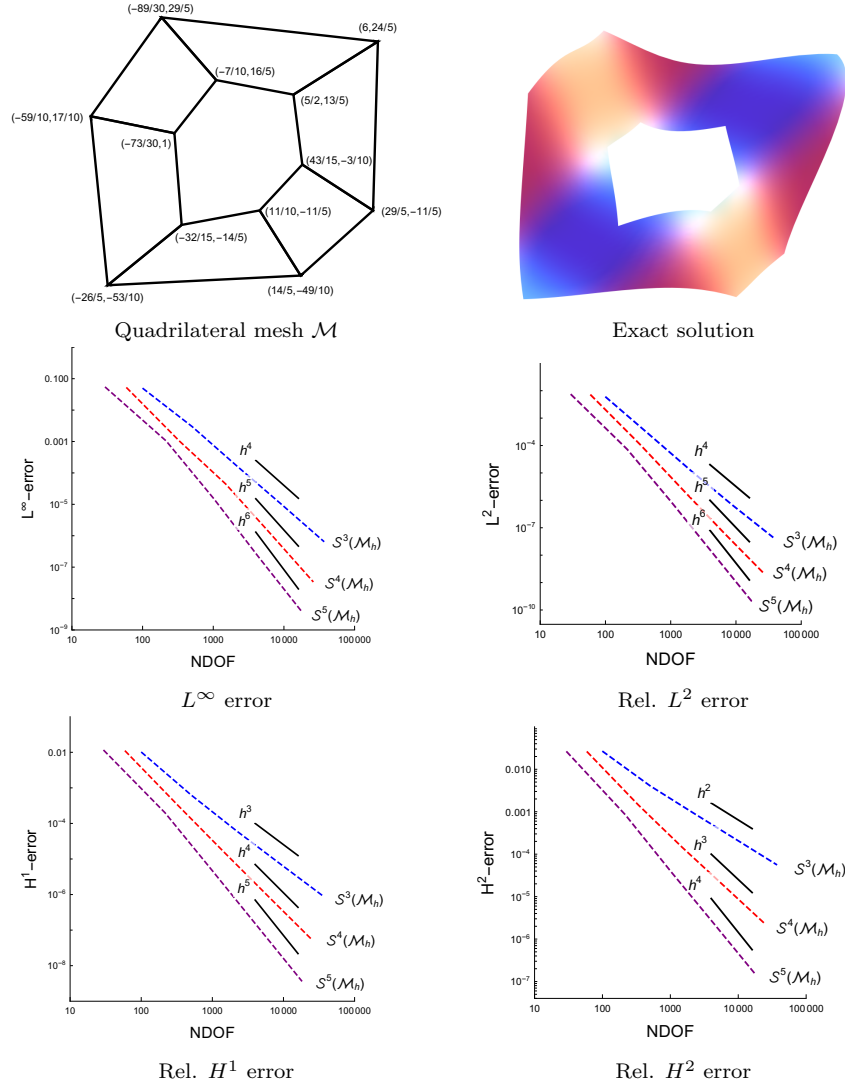


FIGURE 6. Solving the biharmonic equation (8.1) on the given quadrilateral mesh \mathcal{M} (top row, left) for the exact solution (8.2) (top row, right) with the resulting L^∞ and relative L^2 , H^1 , H^2 -errors (middle and bottom row). See Example 8.1.

Example 8.3. In the previous examples the meshes were always nested, even though the spaces were not. Thus, when refining using a regular split, the elements tend to become closer in shape to parallelograms. This is not necessary for optimal convergence, as can be seen in the present example. Here, we reproduce the mesh refinement presented in [2, Figure 1], for the meshes \mathcal{M}_h as depicted in Figure 8 (top row), and solve the biharmonic equation for the exact solution

$$(8.4) \quad u(x_1, x_2) = \frac{1}{4} (x_1^3 + 5x_2^2 - 10x_2^3 + x_2^4)^2$$

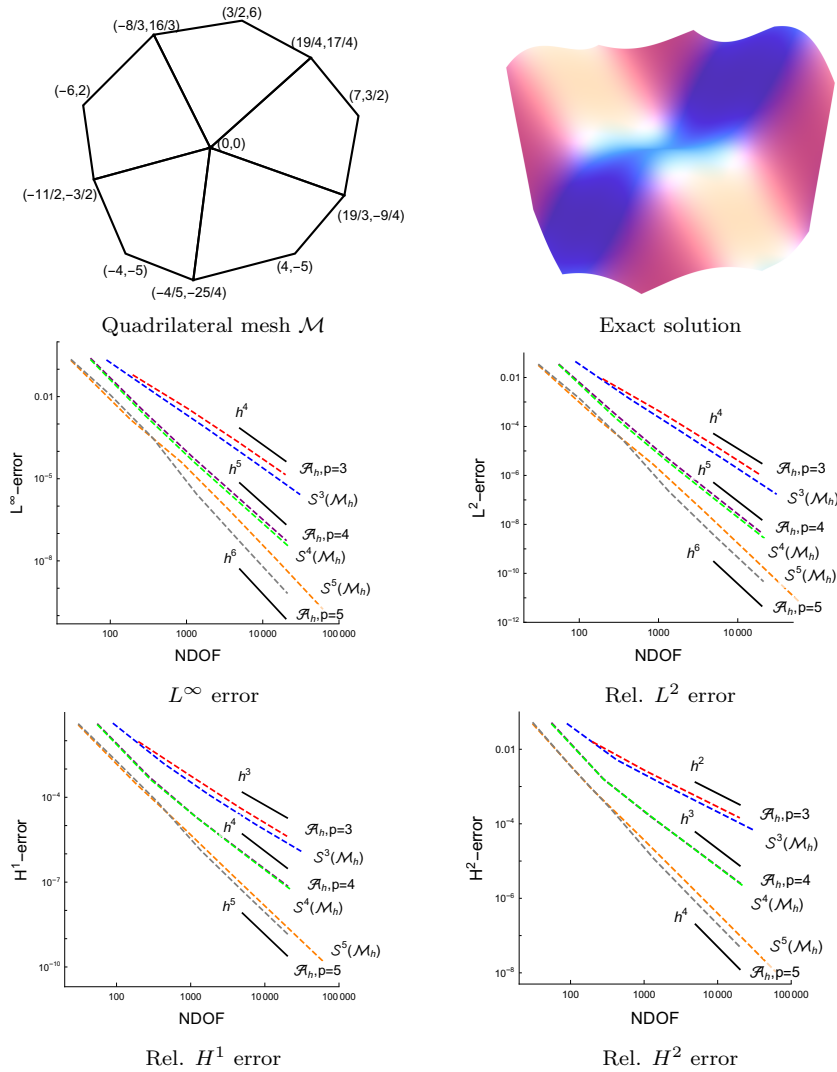


FIGURE 7. Solving the biharmonic equation (8.1) on the given quadrilateral mesh \mathcal{M} (top row, left) for the exact solution (8.3) using the two C^1 -smooth spaces $\mathcal{S}^p(\mathcal{M}_h)$ and \mathcal{A}_h with the resulting L^∞ and relative L^2 , H^1 , H^2 -errors (middle and bottom row). See Example 8.2.

using the space $\mathcal{S}^5(\mathcal{M}_h)$ of degree $p = 5$. In contrast to [2] we introduce local spaces for every element, hence no uniform space on the parameter domain exists. Thus we are guaranteed to reproduce polynomials of degree p , even though not all polynomials of bi-degree (p, p) are present on the parameter domain \widehat{Q} . This is different from [2], where a fixed space of polynomials on the parameter domain (e.g. for the serendipity element) yields optimal convergence rates on the presented mesh if and only if the space contains all polynomials of bi-degree (p, p) .

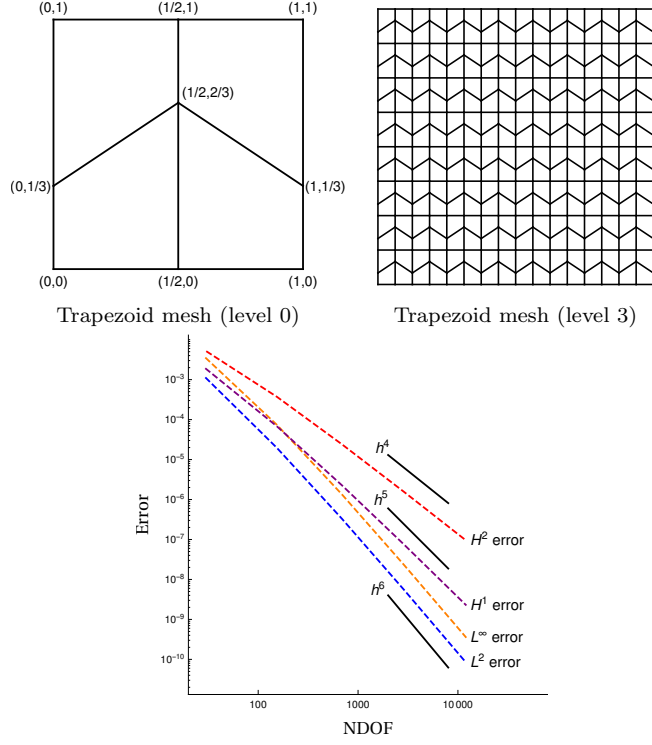


FIGURE 8. Solving the biharmonic equation (8.1) on the given, non-nested quadrilateral meshes \mathcal{M}_h (top row) for the exact solution (8.4) using the C^1 -smooth space $\mathcal{S}^5(\mathcal{M}_h)$ with the resulting L^∞ and relative L^2 , H^1 , H^2 -errors (bottom). See Example 8.3.

Example 8.4. The goal is to compare the BS quadrilateral with the Argyris triangle of degree $p = 5$, comparing the spaces $\mathcal{S}^5(\mathcal{M}_h)$ and $\mathcal{S}^5(\mathcal{T}_h)$, respectively, where \mathcal{T}_h is the resulting refined triangular mesh obtained via splitting each triangle in a regular way into four sub-triangles. For this, we solve the biharmonic equation (8.1) on two different computational domains, where the corresponding quadrilateral and triangular meshes are given in the top rows of Fig. 9 and 10. In our examples, the quadrilateral and triangular meshes possess in each case the same vertices. The considered exact solution is on the one hand

$$(8.5) \quad u(x_1, x_2) = 200 (x_1 x_2 (1 - x_1)(1 - x_2))^2$$

for the computational domain from Fig. 9 (top row, right), and on the other hand

$$(8.6) \quad u(x_1, x_2) = \frac{1}{10^7} \left(\left(\frac{13}{5} - x_2 \right) \left(\frac{26}{5} + \frac{26x_1}{15} - x_2 \right) \left(\frac{26}{5} + \frac{26x_1}{15} + x_2 \right) \right. \\ \left. \left(\frac{13}{5} + x_2 \right) \left(\frac{26}{5} - \frac{26x_1}{15} + x_2 \right) \left(\frac{26}{5} - \frac{26x_1}{15} - x_2 \right) \right)^2.$$

for the computational domain from Fig. 10 (top row, right), and fulfills for both cases homogeneous boundary conditions of order 1. While in Fig. 9 the more regular configuration is used for the quadrilateral mesh compared to the triangular one, it is in the opposite way around for the meshes in Fig. 10. The numerical results, which are shown in the middle and bottom rows of Fig. 9 and Fig. 10, and

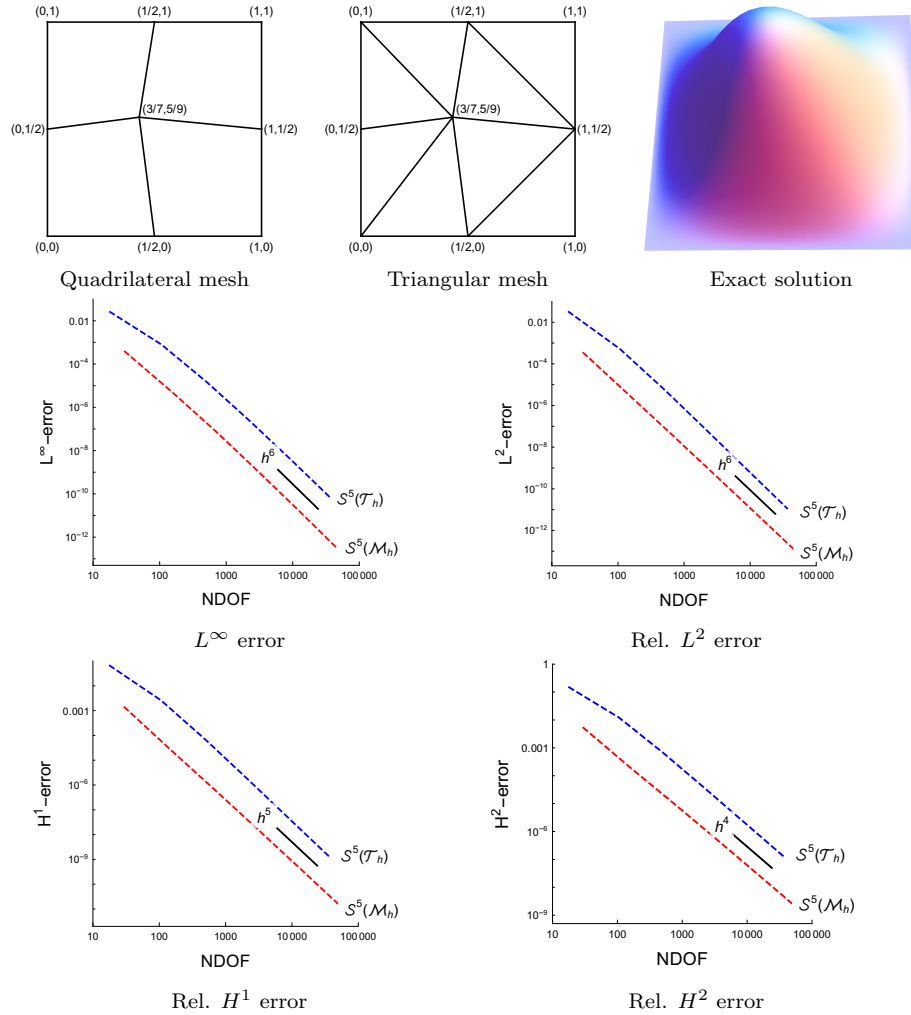


FIGURE 9. Comparison of using the BS quadrilateral spaces $\mathcal{S}^5(\mathcal{M}_h)$ with the Argyris triangle spaces $\mathcal{S}^5(\mathcal{T}_h)$ for solving the biharmonic equation (8.1) on the same computational domain defined either by a quadrilateral (top row, left) or a triangle mesh (top row, middle). Exact solution (8.5) (top row, right) and the resulting L^∞ and relative L^2 , H^1 , H^2 -errors (middle and bottom row). See Example 8.4.

which are compared with respect to the number of degrees of freedom (NDOF), indicate that the BS quadrilateral spaces $\mathcal{S}^5(\mathcal{M}_h)$ perform significantly better than the Argyris triangle spaces $\mathcal{S}^5(\mathcal{T}_h)$ for the more “quad-regular” case (cf. Fig. 9) and just slightly worse for the more “triangle-regular” case (cf. Fig. 10). However, the rates are not affected, as in all considered instances, the resulting L^∞ -error as well as the relative L^2 , H^1 and H^2 -errors decrease with optimal order of $\mathcal{O}(h^6)$, $\mathcal{O}(h^6)$, $\mathcal{O}(h^5)$ and $\mathcal{O}(h^4)$, respectively.

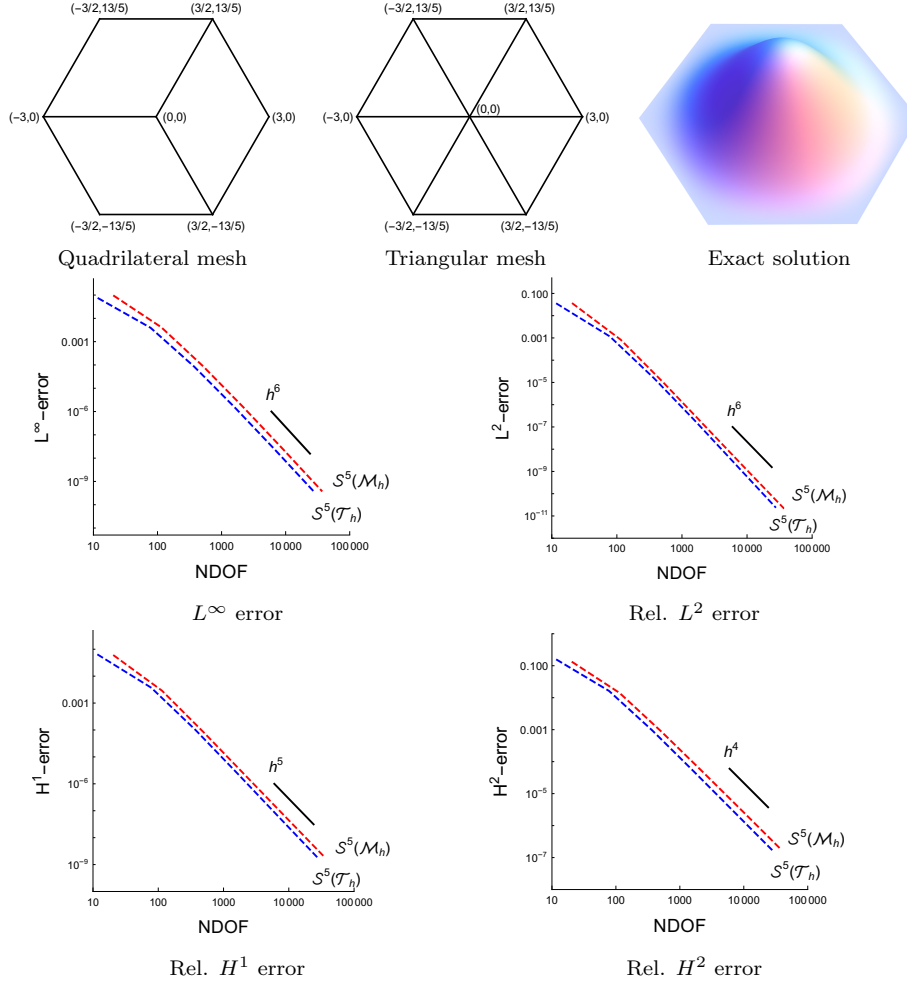


FIGURE 10. Comparison of using the BS quadrilateral spaces $\mathcal{S}^5(\mathcal{M}_h)$ with the Argyris triangle spaces $\mathcal{S}^5(\mathcal{T}_h)$ for solving the biharmonic equation (8.1) on the same computational domain defined either by a quadrilateral (top row, left) or a triangle mesh (top row, middle). Exact solution (8.6) (top row, right) and the resulting L^∞ and relative L^2 , H^1 , H^2 -errors (middle and bottom row). See Example 8.4.

9. CONCLUSION

We have described the construction of a novel family of C^1 quadrilateral finite elements, extending the BS quadrilateral construction from [8], possessing similar degrees of freedom as the classical Argyris triangle [1]. The presented method allows the simple design of polynomial as well as of spline elements. Among others, we have introduced a simple and local basis for the C^1 quadrilateral space, and have stated for particular cases explicit formulas for the Bézier or spline coefficients of the basis functions. We have also studied several properties of the C^1 quadrilateral

space such as the optimal approximation properties of the space. Furthermore, the C^1 quadrilateral spaces are perfectly suited for solving fourth order PDEs, which has been demonstrated on the basis of several numerical examples solving the biharmonic equation on different quadrilateral meshes.

Since the classical Argyris triangle space and the BS quadrilateral space (and variants) presented here possess similar degrees of freedom, we are currently working on an approach to combine the C^1 triangle and quadrilateral element to construct a C^1 element for a mixed triangle and quadrilateral mesh. Further topics which are worth to study are e.g. the use of the C^1 quadrilateral elements for solving other fourth order PDEs such as the Kirchhoff plate problem, the Navier-Stokes-Korteweg equation, problems of strain gradient elasticity, and the Cahn-Hilliard equation, or the extension of our approach to quadrilateral meshes with curved boundaries.

ACKNOWLEDGMENTS

The research of G. Sangalli is partially supported by the European Research Council through the FP7 Ideas Consolidator Grant *HIGEOM* n.616563, and by the Italian Ministry of Education, University and Research (MIUR) through the “Dipartimenti di Eccellenza Program (2018-2022) - Dept. of Mathematics, University of Pavia”. The research of M. Kapl is partially supported by the Austrian Science Fund (FWF) through the project P 33023. The research of T. Takacs is partially supported by the Austrian Science Fund (FWF) and the government of Upper Austria through the project P 30926-NBL. This support is gratefully acknowledged.

REFERENCES

- [1] J. H. Argyris, I. Fried, and D. W. Scharpf, *The TUBA family of plate elements for the matrix displacement method*, The Aeronautical Journal **72** (1968), no. 692, 701–709.
- [2] D. Arnold, D. Boffi, and R. Falk, *Approximation by quadrilateral finite elements*, Mathematics of computation **71** (2002), no. 239, 909–922.
- [3] K. Bell, *A refined triangular plate bending finite element*, International Journal for Numerical Methods in Engineering **1** (1969), no. 1, 101–122.
- [4] M. Bercovier and T. Matskewich, *Smooth Bézier surfaces over unstructured quadrilateral meshes*, Lecture Notes of the Unione Matematica Italiana, Springer, 2017.
- [5] A. Blidia, B. Mourrain, and N. Villamizar, *G^1 -smooth splines on quad meshes with 4-split macro-patch elements*, Computer Aided Geometric Design **52–53** (2017), 106–125.
- [6] F. K. Bogner, R. L. Fox, and L. A. Schmit, *The generation of interelement compatible stiffness and mass matrices by the use of interpolation formulae*, Proc. Conf. Matrix Methods in Struct. Mech., AirForce Inst. of Tech., Wright Patterson AF Base, Ohio, 1965.
- [7] S. C. Brenner and R. Scott, *The mathematical theory of finite element methods*, vol. 15, Springer Science & Business Media, 2007.
- [8] S. C. Brenner and L.-Y. Sung, *C^0 interior penalty methods for fourth order elliptic boundary value problems on polygonal domains*, Journal of Scientific Computing **22** (2005), no. 1-3, 83–118.
- [9] F. Buchegger, B. Jüttler, and A. Mantzaflaris, *Adaptively refined multi-patch B-splines with enhanced smoothness*, Applied Mathematics and Computation **272** (2016), 159 – 172.
- [10] C.L. Chan, C. Anitescu, and T. Rabczuk, *Isogeometric analysis with strong multipatch C^1 -coupling*, Computer Aided Geometric Design **62** (2018), 294–310.
- [11] ———, *Strong multipatch C^1 -coupling for isogeometric analysis on 2D and 3D domains*, Comput. Methods Appl. Mech. Engrg. **357** (2019), 112599.
- [12] P. G. Ciarlet, *The finite element method for elliptic problems*, vol. 40, Siam, 2002.
- [13] A. Collin, G. Sangalli, and T. Takacs, *Analysis-suitable G^1 multi-patch parametrizations for C^1 isogeometric spaces*, Computer Aided Geometric Design **47** (2016), 93 – 113.

- [14] J. A. Cottrell, T.J.R. Hughes, and Y. Bazilevs, *Isogeometric analysis: Toward integration of CAD and FEA*, John Wiley & Sons, Chichester, England, 2009.
- [15] P. Fischer, M. Klassen, J. Mergheim, P. Steinmann, and R. Müller, *Isogeometric analysis of 2D gradient elasticity*, *Comput. Mech.* **47** (2011), no. 3, 325–334.
- [16] H. Gómez, V. M Calo, Y. Bazilevs, and T. J.R. Hughes, *Isogeometric analysis of the Cahn–Hilliard phase-field model*, *Computer Methods in Applied Mechanics and Engineering* **197** (2008), no. 49, 4333–4352.
- [17] H. Gómez, T. J.R. Hughes, X. Nogueira, and V. M. Calo, *Isogeometric analysis of the isothermal Navier–Stokes–Korteweg equations*, *Computer Methods in Applied Mechanics and Engineering* **199** (2010), no. 25, 1828–1840.
- [18] J. A. Gregory and J. M. Mahn, *Geometric continuity and convex combination patches*, *Computer Aided Geometric Design* **4** (1987), no. 1-2, 79–89.
- [19] S. Hahmann and G.-P. Bonneau, *Triangular G^1 interpolation by 4-splitting domain triangles*, *Computer Aided Geometric Design* **17** (2000), 731–757.
- [20] T. J. R. Hughes, J. A. Cottrell, and Y. Bazilevs, *Isogeometric analysis: CAD, finite elements, NURBS, exact geometry and mesh refinement*, *Computer Methods in Applied Mechanics and Engineering* **194** (2005), no. 39-41, 4135–4195.
- [21] Bert Jüttler, *The dual basis functions for the Bernstein polynomials*, *Advances in Computational Mathematics* **8** (1998), no. 4, 345–352.
- [22] M. Kapl, F. Buchegger, M. Bercovier, and B. Jüttler, *Isogeometric analysis with geometrically continuous functions on planar multi-patch geometries*, *Computer Methods in Applied Mechanics and Engineering* **316** (2017), 209 – 234.
- [23] M. Kapl, G. Sangalli, and T. Takacs, *Dimension and basis construction for analysis-suitable G^1 two-patch parameterizations*, *Computer Aided Geometric Design* **52–53** (2017), 75 – 89.
- [24] ———, *Construction of analysis-suitable G^1 planar multi-patch parameterizations*, *Computer-Aided Design* **97** (2018), 41 – 55.
- [25] ———, *Isogeometric analysis with C^1 functions on unstructured quadrilateral meshes*, *The SMAI journal of computational mathematics* **5** (2019), 67–86.
- [26] ———, *An isogeometric C^1 subspace on unstructured multi-patch planar domains*, *Computer Aided Geometric Design* **69** (2019), 55–75.
- [27] M. Kapl, V. Vitrih, B. Jüttler, and K. Birner, *Isogeometric analysis with geometrically continuous functions on two-patch geometries*, *Computers and Mathematics with Applications* **70** (2015), no. 7, 1518 – 1538.
- [28] K. Karčiauskas, T. Nguyen, and J. Peters, *Generalizing bicubic splines for modeling and IGA with irregular layout*, *Computer-Aided Design* **70** (2016), 23–35.
- [29] K. Karčiauskas and J. Peters, *Refinable G^1 functions on G^1 free-form surfaces*, *Computer Aided Geometric Design* **54** (2017), 61–73.
- [30] ———, *Refinable bi-quartics for design and analysis*, *Computer-Aided Design* (2018), 204–214.
- [31] J. Kiendl, Y. Bazilevs, M.-C. Hsu, R. Wüchner, and K.-U. Bletzinger, *The bending strip method for isogeometric analysis of Kirchhoff-Love shell structures comprised of multiple patches*, *Computer Methods in Applied Mechanics and Engineering* **199** (2010), no. 35, 2403–2416.
- [32] J. Kiendl, K.-U. Bletzinger, J. Linhard, and R. Wüchner, *Isogeometric shell analysis with Kirchhoff-Love elements*, *Computer Methods in Applied Mechanics and Engineering* **198** (2009), no. 49, 3902–3914.
- [33] M.-J. Lai and L. L. Schumaker, *Spline functions on triangulations*, Cambridge University Press, 2007.
- [34] T. Matskewich, *Construction of c^1 surfaces by assembly of quadrilateral patches under arbitrary mesh topology*, Ph.D. thesis, Hebrew University of Jerusalem, 2001.
- [35] B. Mourrain, R. Vidunas, and N. Villamizar, *Dimension and bases for geometrically continuous splines on surfaces of arbitrary topology*, *Computer Aided Geometric Design* **45** (2016), 108 – 133.
- [36] T. Nguyen, K. Karčiauskas, and J. Peters, *C^1 finite elements on non-tensor-product 2d and 3d manifolds*, *Applied Mathematics and Computation* **272** (2016), 148 – 158.
- [37] T. Nguyen and J. Peters, *Refinable C^1 spline elements for irregular quad layout*, *Computer Aided Geometric Design* **43** (2016), 123 – 130.

- [38] J. Niiranen, S. Khakalo, V. Balabanov, and A. H. Niemi, *Variational formulation and isogeometric analysis for fourth-order boundary value problems of gradient-elastic bar and plane strain/stress problems*, *Comput. Methods Appl. Mech. Engrg.* **308** (2016), 182–211.
- [39] J. Peters, *Smooth mesh interpolation with cubic patches*, *Computer-Aided Design* **22** (1990), no. 2, 109 – 120.
- [40] ———, *Smooth interpolation of a mesh of curves*, *Constructive Approximation* **7** (1991), no. 1, 221–246.
- [41] ———, *Geometric continuity*, *Handbook of computer aided geometric design*, North-Holland, Amsterdam, 2002, pp. 193–227.
- [42] H. Prautzsch, W. Boehm, and M. Paluszny, *Bézier and B-spline techniques*, Springer, New York, 2002.
- [43] U. Reif, *Biquadratic G-spline surfaces*, *Computer Aided Geometric Design* **12** (1995), no. 2, 193–205.
- [44] G. Sangalli, T. Takacs, and R. Vázquez, *Unstructured spline spaces for isogeometric analysis based on spline manifolds*, *Computer Aided Geometric Design* **47** (2016), 61–82.
- [45] L. L. Schumaker, *Spline functions: Basic theory*, Cambridge University Press, Cambridge, 2007.
- [46] M.A. Scott, D.C. Thomas, and E.J. Evans, *Isogeometric spline forests*, *Comp. Methods Appl. Mech. Engrg.* **269** (2014), 222–264.
- [47] A. Tagliabue, L. Dedè, and A. Quarteroni, *Isogeometric analysis and error estimates for high order partial differential equations in fluid dynamics*, *Computers & Fluids* **102** (2014), 277 – 303.
- [48] D. Toshniwal, H. Speleers, and T. J. R. Hughes, *Smooth cubic spline spaces on unstructured quadrilateral meshes with particular emphasis on extraordinary points: Geometric design and isogeometric analysis considerations*, *Computer Methods in Applied Mechanics and Engineering* **327** (2017), 411–458.

JOHANN RADON INSTITUTE FOR COMPUTATIONAL AND APPLIED MATHEMATICS, AUSTRIAN ACADEMY OF SCIENCES, AUSTRIA

E-mail address: `mario.kapl@ricam.oeaw.ac.at`

DIPARTIMENTO DI MATEMATICA “F. CASORATI”, UNIVERSITÀ DEGLI STUDI DI PAVIA, ITALY;
ISTITUTO DI MATEMATICA APPLICATA E TECNOLOGIE INFORMATICHE “E. MAGENES” (CNR), ITALY

E-mail address: `giancarlo.sangalli@unipv.it`

INSTITUTE OF APPLIED GEOMETRY, JOHANNES KEPLER UNIVERSITY LINZ, AUSTRIA

E-mail address: `thomas.takacs@jku.at`